

Received September 21, 2019, accepted October 7, 2019, date of publication October 11, 2019, date of current version October 29, 2019.

Digital Object Identifier 10.1109/ACCESS.2019.2947009

# Determination of Neural Network Parameters for Path Loss Prediction in Very High Frequency Wireless Channel

SEGUN I. POPOOLA<sup>1,2</sup>, ABIGAIL JEFIA<sup>2</sup>, ADEREMI A. ATAYERO<sup>2</sup>, OGBEIDE KINGSLEY<sup>3</sup>, NASIR FARUK<sup>4</sup>, OLASUNKANMI F. OSENI<sup>5</sup>, AND ROBERT O. ABOLADE<sup>5</sup>

<sup>1</sup>Department of Engineering, Manchester Metropolitan University, Manchester M1 5GD, U.K.

<sup>2</sup>Department of Electrical and Information Engineering, Covenant University, Ota 1023, Nigeria

<sup>3</sup>Department of Electrical and Information Engineering, Landmark University, Omu-Aran 1001, Nigeria

<sup>4</sup>Department of Telecommunication Science, University of Ilorin, Ilorin 1515, Nigeria

<sup>5</sup>Department of Electronic and Electrical Engineering, Ladoko Akintola University of Technology, Ogbomosho 4000, Nigeria

Corresponding author: Segun I. Popoola (s.popoola@mmu.ac.uk)

This work was supported by the IoT-Enabled Smart and Connected Communities (SmartCU) Research Cluster of Covenant University and the Covenant University Center for Research, Innovation and Discovery (CUCRID), Nigeria.


**ABSTRACT** It is very important to understand the input features and the neural network parameters required for optimal path loss prediction in wireless communication channels. In this paper, an extensive investigation was conducted to determine the most appropriate neural network parameters for path loss prediction in Very High Frequency (VHF) band. Field measurements were conducted in an urban propagation environment to obtain relevant geographical and network information about the receiving mobile equipment and quantify the path losses of radio signals transmitted at 189.25 MHz and 479.25 MHz. Different neural network architectures were trained with varying kinds of input parameters, number of hidden neurons, activation functions, and learning algorithms to accurately predict corresponding path loss values. At the end of the experimentations, the performance of the developed Artificial Neural Network (ANN) models are evaluated using the following statistical metrics: Mean Absolute Error (MAE), Mean Squared Error (MSE), Root Mean Squared Error (RMSE), Standard Deviation (SD) and Regression coefficient (R). Results obtained show that the ANN model that yielded the best performance employed four input variables (latitude, longitude, elevation, and distance), nine hidden neurons, hyperbolic tangent sigmoid (tansig) activation function, and the Levenberg-Marquardt (LM) learning algorithm with MAE, MSE, RMSE, SD and R values of 0.58 dB, 0.66 dB, 0.81 dB, 0.56 dB and 0.99 respectively. Finally, a comparative analysis of the developed model with Hata, COST 231, ECC-33 and Egli models showed that ANN-based path loss model has better prediction accuracy and generalization ability than the empirical models.

**INDEX TERMS** Artificial neural network, path loss, radio propagation, wireless channel, machine learning.

## I. INTRODUCTION

Wireless communication is fast evolving with diverse disruptive enabling technologies, thereby leading to a serious demand for high quality signal strength and larger network capacity [1]. Information and Communication Technology (ICT) has been identified as a veritable tool for the achievement of Sustainable Development Goals (SDGs) by 2030 [2]. However, wireless connectivity and coverage required for sustainable digital transformation is still not

globally available; and this poses a challenge to the timely accomplishment of the desired SDGs. With this in mind, it is evident that the extension of the wireless connectivity and coverage to the yet-to-be-reached population would facilitate global digital transformation, thus providing the necessary technology required for the development of ICT services in the underserved areas. In a bid to design efficient wireless communication systems, the propagation factors affecting the radio channel often pose serious challenges to radio network engineers whose responsibility is to ensure that subscribers are provided with high speed Internet services at optimum Received Signal Strength (RSS) [3]. For such

The associate editor coordinating the review of this manuscript and approving it for publication was Francesco Mercardo .

efficient network design to be achieved, accurate and reliable path loss models are highly essential for radio network coverage and signal interference predictions.

Path loss is a form of signal fading which occurs due to attenuation of signal power between the receiving and transmitting stations [4]. The signal attenuation is mainly due to physical propagation mechanisms such as reflection, refraction, diffraction and scattering. Prediction models can be used to determine the most suitable location for wireless communication system deployment [5]. Improper placement of base stations in a wireless system will result in poor network performance and low Quality of Service (QoS). It is, therefore, helpful to develop an optimal path loss prediction model for the design of efficient and effective wireless communication systems. Moreover, radio network engineers have no control over the physical obstructions in the wireless channel. The simple solution is to correctly account for all losses in the wireless channel during radio network planning and optimization processes.

Radio propagation models are mathematical functions that characterize radio wave propagation in a given environment based on certain terrain and network information about the transmitter, the receiver and the propagation environment. Deterministic propagation models are based on physical laws of wave propagation [6] and they produce accurate prediction results but with high computational complexity. On the other hand, empirical propagation models are simpler and easier to use because they are dependent on observations and measurements carried out in a given environment [7]. However, they tend to produce higher prediction errors than deterministic models.

Machine learning is a technique aimed at improving system performance based on a flexible model architecture and good amount of appropriate data. Recently, machine learning has gained recognition in several fields including autonomous driving, computer vision, speech recognition etc. Previous studies have considered the suitability of different machine learning techniques for path loss prediction [8]–[12].

Artificial Neural Network (ANN) is an adaptive system which makes modifications to its structure and response characteristics in the course of a training process [13]. The ideology behind the neural network is derived from the biological nervous system. ANNs are referred to as adaptive statistical tools which are capable of modeling the behavior of the biological nervous systems in information processing. ANN behaves in a similar way to human beings in the sense that, with the aid of some examples related to a given process, they are able to represent that process. In essence, ANN learns by example. Due to their flexibility and simplicity, their applications in tough areas (such as pattern recognition, regression) have proven to be successful in several fields like physics, medicine, engineering, statistics and econometrics. A suitable algorithm is employed for training the preferred model in a controlled manner, bearing the generalization factor in mind. Generalization in a neural network occurs when developed ANN model demonstrate the ability to properly

obtain the input-output mapping for test data excluded from the training data set. In general, the generalization ability of a neural network is strictly associated its complex-ability. In fact, the more complex a network is, the poorer its process approximation on points not included in the training set (that is, the testing set). The phenomenon is regarded as *overfitting*. However, a simple model is also not ideal due to its inability to provide a good fit to the training data.

The idea of ANN was introduced to path loss predictions with the aim of overcoming the shortcomings of the empirical and deterministic models [8]. ANN models have proven to be easier to deploy than deterministic models and they are also more accurate than empirical models [14]. In addition, ANN can be adapted for path loss predictions in rural, suburban and urban propagation environments. Basically, path loss prediction is classified as a regression problem. In this case, ANN model is trained with field measured data to understand the non-linear relationship between the output variable (path loss) and the dependent/input variables such as the frequency of transmission, building height, receiver antenna height, transmitter antenna height, separation distance between the base station and the mobile station etc. Determination of the appropriate input/feature vector and the correct setting of neural network parameters needed for optimal path loss prediction is very crucial. This is the motivation for this present study. The rest of the paper is organized as follows: Section II presents the review of related work and main contributions; Section III presents the measurement set-up and data collection process as well as the training, validation and testing of ANN models; Section IV presents and discusses results obtained from the experimentations; and Section V concludes the paper.

## II. REVIEW OF RELATED WORK AND MAIN CONTRIBUTIONS

Many researchers have developed ANN models for path loss predictions. Piacentini and Rinaldi [15] proposed the use of machine learning and dimensionality reduction techniques for path loss prediction. The authors assessed the effects of dimensionality reduction on path loss prediction accuracy. Also, the abilities of ANN and Support Vector Machines (SVM) to efficiently solve the regression problem were examined. For the ANN model, a two-layered multilayer perceptron was selected as the neural network architecture and its generalization ability was evaluated using *cross-validation* technique. SVMs were trained using *Library for Support Vector Machines (LIBSVM)* while *Fortran 90* was used to implement the algorithms for dimensionality reduction techniques. It was reported that dimensionality reduction improved the prediction accuracy of the machine learning models but ANN yielded better results than SVM.

Eichie *et al.* [16] and Popescu *et al.* [17] investigated the analysis of empirical models and ANN model for path loss prediction. The ANN inputs were propagation parameters and the radio network data were acquired through drive test along preferred suburban and rural routes. The prediction

results of the ANN model were compared with the ones obtained based on the use of basic empirical path loss models namely: Egli, COST-231, Hata and Ericsson models. ANN-based path loss model yielded better results when compared to basic models. The authors concluded that ANN model is useful for accurate path loss prediction in rural and suburban propagation environments.

Cerri *et al.* [18] suggested the use of Multi-Layer Perceptron (MLP) for path loss prediction in urban areas. ANN was trained using backpropagation (BP) algorithm. Comparison of results with analytical models showed that the proposed method is efficient for radio network planning and optimization. Sotiroidis and Siakavara [19] also proposed the use of ANN models for prediction of path loss in urban areas. Their work seems similar to other general research works but they aimed at discovering the needed amount and kind of information to be used as network inputs. The network input information is the terrain profile of the propagation environment and the data provided is of minimal amount. The results of the proposed ANN model proved that the model was capable of predicting path loss in urban (randomly-built) environment. More importantly, working with a small number of inputs with detailed specifications of the propagation also yielded significant accuracy, which turned to be better than previously proposed ANN methodologies. The work revealed that the developed model is effective in performing path loss prediction.

Sotiroidis *et al.* [20] provided an alternative approach for the prediction of path loss in urban areas by applying a Differential Evolution (DE) algorithm, called Composite DE (CoDE) in developing an optimal ANN. The authors proposed a methodology for achieving optimum ANN. The results of CoDE were compared with those obtained from various DE strategies. It was reported that CoDE was highly effective with the advantages of being easy to implement and modifiable. Also, two ANN architectures with two and three hidden layers were evaluated using CoDE, and the performance proved their effectiveness and accuracy in yielding expected results. The final results were compared with results yielded by ray-tracing model, and the proposed method showed better accuracy. Further work was recommended to improve generalization and approximation abilities of the ANN by utilizing data sets for non-uniform built-up environments.

Kalakh *et al.* [21] developed a neural network model for Ultra-Wide Band (UWB) channel path loss in a mine environment. The authors aimed at presenting this model with a focus on alterations in path loss attenuation with respect to time and distance. Neural network model was built using the MLP architecture while employing the backpropagation algorithm for the training. The results obtained from the neural network training and testing were compared with experimental measured values. The neural network model correctly predicted the changes in the path loss attenuation, while providing sufficient accuracy with the experimental measurements. The work revealed the significance and efficiency of

neural networks for path loss prediction in a typical harsh environment (in this case, a mine).

Popescu *et al.* [22] also applied neural networks for the prediction of path loss in urban environments, but in this case, two separate neural network models were considered for Line-of-Sight (LOS) and Non-Line-of-Sight (NLOS) cases. In the LOS case, relevant data (including transmitter and receiver distance, height of buildings, streets width, separation of building and transmitting antenna position with respect to the rooftop) were used to train the ANN model. For the NLOS case, two ANN models were built. The first model was trained with the same parameters from the LOS case while the second model was built with the same parameters, also including diffraction losses computed by COST231-Walfisch-Ikegami algorithm. The “hybrid network”, which combined path loss algorithms, network data and the neural network approach, yielded better results with acceptable accuracy.

Ostlin *et al.* [14] suggested the use of ANN for macrocell path loss prediction. In order to train and test the model, data obtained from a commercial code division multiple access were used. The feed-forward neural network architecture was used alongside two backpropagation algorithms namely: Levenberg-Marquardt (LM) and Scale Conjugate Gradient (SCG). Base station distance, vegetation type, land usage, terrain path profile parameters and density near receiving antenna were used as the inputs. The path loss prediction results from the ANN model were compared with two other propagation models (Recommendation ITU-R P.1546 and the Okumura-Hata model) to reveal that the trained ANN model produced results with better accurate prediction. Although the research work yielded good results, large path loss changes could not be predicted as there was an absence of databases for the topography. However, they authors proposed future work, which would include specified training data with a wider range of the propagation problem, thereby improving generalization properties and accuracy of the neural network model.

Liu *et al.* [23] proposed an Single Hidden Layer Feedforward Neural Network (SHLFFNN) method for the modelling of fading channels (path loss prediction), including small-scale variation and large-scale attenuation. For small-scale variation, two algorithms (ELM and LM) were employed in training the neural network and the results showed that ELM was as effective as the BP algorithm. For large-scale attenuation, the ELM estimator required for the path loss prediction exponent was established and it yielded results with higher speed when compared to the BP algorithm. These results proved the effectiveness of the ELM algorithm in the neural network model.

Zaarour *et al.* [24] present an experimental study for modelling path loss in UWB channel in a mine environment by implementing Radial Basis Function (RBF) and MLP with a focus on variations in path loss attenuation with respect to distance and frequency. This was considered a different approach in path loss modeling in a mine environment.

The results obtained showed the efficiency of the RBF in modeling path loss as it provided a lower error rate and higher accuracy in path loss prediction. The authors concluded that the research work would help in determining the best ANN type for modeling the channel in a mine environment.

Fernández Anitzine *et al.* [25] provided an analysis based on ANNs for the prediction of path loss in both indoor and outdoor links. They aimed at providing a means of properly selecting training set for the development of an effective ANN model, which entailed the use of the LM algorithm for the training process. The authors focused on implementing a simplified ray-tracing tool (for the identification of the “dominant path”), combined with ANN inputs derived from the calculation of a number of propagation parameters. The results of the training were compared with measurements different from those used in the training process, and it proved that ANN was more accurate, as its input parameters, which were acquired from the ray-tracer were similar for adjacent points along the route. In addition, a complete and detailed description of the training process was presented, with a focus on selecting an optimum training dataset.

Zineb and Ayadi [26] developed a new propagation model using ANN. Neural networks and data mining techniques were combined to develop a new model. The proposed model, derived from the multi-wall model was intended for the most popular frequency bands including UMTS, GSM and WiFi. The neural network was modelled using MLP framework, and it was trained with measured data (including frequency, floor attenuation, transmitter-receiver distance and frequency) utilizing the BP learning algorithm. The results derived from the ANN-based multi-wall multi-frequency (ANN-based MWMF) model showed better performance and higher accuracy as compared to a calibrated multi-wall model. The authors suggested that the results obtained could be improved by including other parameters, not contained in the model e.g. diffraction loss, body shadowing, and so on.

Gómez-Pérez *et al.* [27] recommended the use of ANN for attenuation modeling prompted by vegetation barriers at cellular frequency bands of 2G to 4G. MLP architecture was used, and trained with measurements of various configurations of vegetation barriers (such as barrier thickness, vegetation density, foliage, polarization, frequency, trunk density of vegetation specie and receiver position along the linear rail) as well as vegetation species at frequency bands of 900, 1800 and 2100MHz. After training and testing, comparisons were carried out with the obtained inferred attenuation of the ANN and the experimental data. In addition, various inferred attenuations were compared, where the obtained ANN results were also compared with path loss obtained by ITU-R recommendation and linear regression. As a result of these comparisons, it was shown that the model was highly efficient in predicting accurate attenuation in the specified frequency bands, while retaining low median error. It was suggested that the model would be highly beneficial to radio network planners in predicting the attenuation caused by vegetation formation. However, the frequency bands used in this model

can be extended to higher frequencies (such as Wi-Fi, Wi-Max or 5G frequency bands), provided appropriate training is carried out.

Popoola *et al.* [9] established an optimal model for the prediction of path loss utilizing feed-forward neural networks. In order to obtain input data, drive test measurements were conducted at varying distances from several base station transmitters. SHLFNN was trained with the derived data (including elevation, clutter height, longitude, altitude, latitude) using LM algorithm. Afterwards, the ANN model performance was evaluated. The results derived from model were compared with popular empirical models (COST231, Egli, Hata and ECC-33) [7], [28], [29] to reveal the optimal performance of the ANN model in improving accuracy and generalization ability. In future, more data can be sourced from various propagation environments and other machine learning techniques can be exploited as well.

Eichie *et al.* [30] established a model based on neural networks for the determination of GSM RSS level with the use of atmospheric factors (e.g. relative humidity, atmospheric temperature, dew point). These atmospheric factors were used as the inputs for the ANN model and trained with the aid of the LM algorithm. The development of the model was a three-step approach. Firstly, the required data were acquired; then the data collected were pre-processed; finally, the proposed ANN model was designed and implemented using the weight and bias values to form model equation. The results obtained showed that the developed model performed optimally with low MSE and acceptable accuracy values.

Benmus *et al.* [13] proposed the prediction of path loss at 900, 1800, and 2100 MHz bands by means of the neural network approach. They collected measurements from five different areas namely; urban, dense-urban, suburban, dense-suburban and rural areas, at the specified frequency bands, which were used for the model training and evaluation. The results derived from the model were compared with Hata model by evaluating performance based on the MSE. The MSE for the proposed model was lower than that of the Hata model, while maintaining a high level of accuracy.

Bhuvaneshwari *et al.* [31] evaluated three dynamic neural networks namely: Focused Time Delay Neural Network (FTDNN), Distributed Time Delay Neural Network (DTDNN) and Layer Recurrent Neural Network (LRNN) for the path loss prediction in a bid to minimize errors between the measurements and simulations. Each of the dynamic neural networks were trained with LM and SCG training algorithms. Performance evaluation was analyzed with respect to the correlation between measurements and simulations, the ME value and the SD value. Results showed that LRNN provided the best performance with increased computation time, while the FTDNN performed better than the DTDNN.

Angeles and Dadios [32] proposed an alternative ANN model for the prediction of path loss in digital TV macrocells. The model was designed using the Longley-Rice simulation, with the aid of a feedforward neural network architecture



**TABLE 1. Taxonomy of related studies based on network parameter optimization.**

| Ref.              | Varying Input data variables | Varying hidden layer activation function | Varying output layer activation function | Varying learning algorithm | Varying number of hidden neurons |
|-------------------|------------------------------|--|--|----------------------------|----------------------------------|
| [9]               | X                            | X  | X  | X                          | ✓                                |
| [15]              | ✓                            | X  | X  | X                          | X                                |
| [16]              | X                            | ✓  | X  | X                          | ✓                                |
| [17]              | X                            | X  | X  | X                          | X                                |
| [18]              | X                            | X  | X  | X                          | ✓                                |
| [19]              | ✓                            | ✓  | X  | X                          | ✓                                |
| [20]              | X                            | X  | X  | ✓                          | ✓                                |
| [21]              | X                            | X  | X  | X                          | ✓                                |
| [22]              | ✓                            | X  | X  | X                          | ✓                                |
| [14]              | X                            | X  | X  | ✓                          | ✓                                |
| [23]              | X                            | X  | X  | X                          | ✓                                |
| [24]              | X                            | X  | X  | X                          | X                                |
| [25]              | X                            | X  | X  | X                          | X                                |
| [26]              | X                            | X  | X  | X                          | ✓                                |
| [27]              | X                            | X  | X  | X                          | X                                |
| [30]              | X                            | ✓  | X  | ✓                          | ✓                                |
| [13]              | X                            | X  | X  | X                          | X                                |
| [31]              | X                            | ✓  | X  | ✓                          | ✓                                |
| [32]              | X                            | X  | X  | X                          | ✓                                |
| [33]              | ✓                            | X  | X  | X                          | ✓                                |
| [34]              | X                            | X  | X  | X                          | X                                |
| <b>This Study</b> | ✓                            | ✓  | ✓  | ✓                          | ✓                                |

and trained using a BP algorithm. The results derived from the prediction model was of better performance compared to other propagation models such as free space propagation model and the Egli model. The developed model was able to adapt to arbitrary environments. The effects of multiple transmitter locations and the positioning of the receivers higher than a transmitter can be investigated in future work.

Ferreira *et al.* [33] utilized ANN for the purpose of improving the prediction of the outdoor signal strength in the Ultra High Frequency (UHF) band. Measurements were conducted at 1140 MHz in an urban environment, while RSSL was measured using the Delta-Bullington method and Cascade Knife Edge, both available in ITU-R. Input such as transmitter-receiver distance, diffraction loss and signal strength prediction were fed into the ANN, which showed great effectiveness in predicting RSS. The results obtained from the study revealed that ANN can be used as a supplement tool for ITU prediction models.

Ayadi *et al.* [34] developed a UHF path loss model based on neural networks for heterogeneous networks. Conducted measurements were split into two: one for model training while the other was used for model validation. The proposed neural network-based model made use of the BP algorithm, while obtaining inputs from Standard Propagation Model (SPM) and an addition of various parameters such as diffraction loss, type of environment, frequency and land use

**TABLE 2. Taxonomy of related studies based on measurement location and signal frequency.**

| Ref.              | Measurement Location    | Frequency Band | Frequency (MHz)               |
|-------------------|-------------------------|----------------|-------------------------------|
| [9]               | Ota and Ilorin, Nigeria | UHF            | 1800                          |
| [15]              | Munich, Germany         | UHF            | 947                           |
| [16]              | Minna, Nigeria          | UHF            | 1800                          |
| [17]              | Kavala and Oia, Greece  | UHF            | 1890                          |
| [18]              | Simulated               | -              | -                             |
| [19]              | Simulated               | UHF            | 900                           |
| [20]              | Simulated               | -              | -                             |
| [21]              | Val d’Or, Canada        | SHF            | 3000-10000                    |
| [22]              | Kavala, Greece          | UHF            | 1890                          |
| [14]              | Western Australia       | UHF            | 881.52                        |
| [23]              | Simulated               | UHF            | 2350                          |
| [24]              | Val d’Or, Canada        | SHF            | 3000-10000                    |
| [25]              | Simulated               | UHF            | 900 and 1800                  |
| [26]              | Tunis, Tunisia          | UHF            | 900, 1800, 2100 and 2400      |
| [27]              | Simulated               | UHF            | 900, 1800 and 2100            |
| [30]              | Minna, Nigeria          | UHF            | 1835-1850                     |
| [13]              | Tripoli, Libya          | UHF            | 900, 1800 and 2100            |
| [31]              | Hyderabad, India        | UHF            | 947.5                         |
| [32]              | Simulated               | UHF            | 600                           |
| [33]              | Rio de Janeiro, Brazil  | UHF            | 1140                          |
| [34]              | Tunis, Tunisia          | UHF            | 450, 850, 1850, 2100 and 2600 |
| <b>This Study</b> | Benin, Nigeria          | VHF            | 189.25 and 479.25 MHz         |

distribution. Comparison of results from the neural network model with results obtained from SPM and ITU-R models showed the accuracy of the developed model.

In conclusion, the review of related works is organized into four categories of 20 criteria. The details extracted from 21 related articles are presented in Tables 1-4. Category 1 (network parameter optimization) include: (a) varying input data variables; (b) varying hidden layer activation function; (c) varying output layer activation function; (d) varying learning algorithms; and (e) varying number of hidden neurons. Category 2 (measurement location and signal frequency) include: (a) measurement location (city and country); (b) frequency band; and (c) signal frequency. Category 3 (neural network configuration and training parameters) include: (a) input data variables; (b) data pre-processing; (c) activation functions; (d) number of hidden layer and

**TABLE 3. Taxonomy of related studies based on neural network configuration and training parameters.**

| Ref. | Input data variables  | Data pre-processing                      | Activation functions                                    | No of hidden layer and neurons              | Learning Algorithms | Performance Metrics   |
|------|---|--|---|---|---------------------|-----------------------|
| [9]  | Longitude, latitude, Distance, elevation, altitude, clutter height  | Min-max normalization (input)            | tansig  | One (1-50 neurons)                          | LM                  | MAE, MSE, RMSE, SD, R |
| [15] | Distance, portion through building, height, thickness   | Dimensionality reduction (PCA) (input)   | tansig  | One   | L-BFGS              | MSE                   |
| [16] | Distance, elevation, transmitting power   | Min-max normalization (input and output) | logsig, purelin, tansig                                 | One (31-39 neurons)                         | -                   | MSE, RMSE             |
| [17] | Distance, street width, building height, building separation, transmitter position, street orientation, base station antenna and rooftop height difference                                    | -  | -   | One   | -                   | ME, SD, RMSE          |
| [18] | the direct ray, the reflected ray from the ground, the two dominant reflected rays arriving to the receiver after reflections from vertical walls, and the ray diffracted by the last rooftop | Min-max normalization (input)            | -   | Two (1-20 neurons)                          | LM                  | MSE, SD               |
| [19] | Terrain information, coordinates of path loss estimation point  | -  | purelin, tansig   | One   | -                   | MSE, MAE, RMSE        |
| [20] | Coordinates of position, environmental structure  | -  | -   | Case 1: Two<br>Case 2: Three                | LM                  | MAE, RMSE             |
| [21] | Frequency, distance   | -  | tansig, purelin   | One (1-80 neurons)                          | LM                  | MSE                   |
| [22] | Distance, street width, building height, building separation, transmitter position  | Min-max normalization (input)            | -   | LOS: Two (10 neurons)<br>NLOS: Two (18 neu) | LM                  | MSE, SD<br>RMSE       |
| [14] | Distance, antenna height, terrain clearance angle, terrain usage, vegetation type, vegetation density   | -  | Tansig  | Several (numerous neurons)                  | LM                  | ME, SD, R             |
| [23] | -   | -  | tansig  | One (10-20 neurons)                         | LM                  | RMSE                  |
| [24] | Frequency, distance   | -  | MLP: tansig, purelin<br>RBF: Gaussian function, purelin | One   | -                   | MSE                   |

neurons; (e) learning algorithms; and (f) performance metrics. Category 4 (performance evaluation results) include: (a) Mean Error (ME); (b) Mean Absolute Error (MAE);

(c) Mean Square Error (MSE); (d) Root Mean Square Error (RMSE); (e) Standard Deviation (SD) and; (f) Regression Coefficient (R).

TABLE 3. (continued.) Taxonomy of related studies based on neural network configuration and training parameters.

|                   |  |                               |                         |                       |                                 |                           |
|-------------------|--|-------------------------------|-------------------------|-----------------------|---------------------------------|---------------------------|
| [25]              | Indoor: screen effect, local reflection, waveguide effect, change of direction, transmission loss, free space loss<br><br>Outdoor: distance, incidence & scattering angles, reflection & diffraction coefficients, free space loss | -                             | Logsig, purelin         | Two                   | LM                              | ME, MSE, SD               |
| [26]              | Distance, frequency, wall attenuation, floor attenuation   | -                             | Logsig                  | One                   | LM                              | ME, SD                    |
| [27]              | Barrier thickness, vegetation density, position of receiver along guide, polarization, frequency   | Min-max normalization (input) | -                       | One                   | LM                              | RMSE                      |
| [30]              | Temperature, humidity, dew point   | Min-max normalization (input) | Logsig, tansig, purelin | One (33 neurons)      | LM                              | MSE                       |
| [13]              | -  | -                             | -                       | One                   | -                               | RMSE                      |
| [31]              | Frequency, distance, antenna height, correction factor   | Min-max normalization (input) | -                       | One (30 neurons)      | LM, SCG                         | ME, SD, R                 |
| [32]              | Distance, bearing, elevation   | -                             | Tansig, purelin         | One (19 neurons)      | LM                              | SD                        |
| [33]              | Distance, diffraction loss, signal strength prediction   | -                             | -                       | One (10 – 30 neurons) | LM                              | SD                        |
| [34]              | Distance, transmitter & receiver height  | Min-max normalization (input) | Tansig                  | One                   | Back-propagation                | MAE, SD, R                |
| <b>This Study</b> | Latitude, longitude, elevation, distance   | Min-max normalization (input) | Purelin, logsig, tansig | One (1-20 neurons)    | LM, BFG, RP, SCG, CGF, CGP, GDX | ME, MAE, MSE, RMSE, SD, R |

In the process of literature review, 21 related articles were identified and thoroughly reviewed. To the best of our knowledge:

Table 1 shows that there is no single study that performed extensive neural network parameter optimization to guarantee high model accuracy and better generalization ability. In this new study, different ANN parameters were optimized to minimize path loss prediction error. The optimization experimentations include varying the: (a) input data variables; (b) hidden layer activation function; (c) output layer activation function; (d) learning algorithms; and (e) number of hidden neurons.

Table 2 shows that previous ANN modelling in the literature employed measurement data that were collected from radio networks which transmit signals at frequencies above Very High Frequency (VHF) band. Meanwhile, VHF signal

range is 30-300 MHz. However, majority of the reviewed work focused on UHF networks [9], [15]–[17], [19], [14], [22], [23], [13], [25]–[34]; two studies focused on Super High Frequency (SHF) network [21], [24]; while the remaining seven studies employed simulated data for ANN-based path loss modelling [18]–[20], [23], [25], [27], [32]. Given the same propagation environment, the behaviour of radio signals often changes with varying transmission frequency. Also, only two of the 21 studies were conducted to capture the unique features of Nigerian propagation terrain. However, these studies focused on a different city other than the one selected for this present study. Therefore, this present study seeks to develop ANN model for path loss predictions based on real data obtained from a typical VHF radio network operating at 189.25 MHz in an urban propagation environment (Benin City, Nigeria).

**TABLE 4.** Taxonomy of related studies based on performance evaluation results.

| Ref.              | ME (dB)   | MAE (dB)  | MSE (dB)   | RMSE (dB)   | SD (dB)   | R   |
|-------------------|---|---|--|---|---|---|
| [9]               | -   | 4.21 (Tr)<br>4.74 (Te)  | 30.99 (Tr)<br>39.38 (Te)   | 5.56 (Tr)<br>6.27 (Te)  | 5.56 (Tr)<br>6.27 (Te)  | 0.89 (Tr)<br>0.86 (Te)  |
| [15]              | -   | -   | 53.25  | -   | -   | -   |
| [16]              | -   | -   | -  | 1.22-7.07   | -   | -   |
| [17]              | 3.67-5.08   | -   | -  | 3.71-6.78   | 2.46-4.65   | -   |
| [18]              | -   | 0.71  | -  | -   | 1.0   | -   |
| [19]              | -   | 2.74-5.59   | -  | 3.54-6.98   | -   | -   |
| [20]              | -   | 1.84-1.97   | -  | 2.41-2.49   | -   | -   |
| [21]              | -   | -   | 1.04 (Tr1)<br>1.04 (Tr2)<br>4.0 (Tr3)<br>1.12 (Tr4)<br>6.76 (Te)                                 | -   | -   | -   |
| [22]              | 1.65-5.04   | -   | -  | 2.13-6.63   | 1.35-4.71   | -   |
| [14]              | 0   | -   | -  | -   | 7.00  | -   |
| [23]              | -   | -   | -  | 0.28  | -   | -   |
| [24]              | -   | -   | 1.76   | -   | -   | -   |
| [25]              | -   | -   | 1.77-8.78  | 2.52-9.34   | 1.79-8.00   | -   |
| [26]              | 0.75  | -   | -  | -   | 5.22  | 0.96  |
| [27]              | -   | -   | -  | 0.57  | -   | -   |
| [30]              | -   | -   | 0.06   | -   | -   | -   |
| [13]              | -   | -   | -  | 3.0 – 6.7   | -   | -   |
| [31]              | -   | -   | -  | -   | 11.37   | 0.99  |
| [32]              | -   | -   | 94.58  | -   | -   | -   |
| [33]              | -   | -   | -  | -   | 2.86-3.81   | -   |
| [34]              | -   | 0.24  | -  | -   | 6.85  | 0.85  |
| <b>This Study</b> | 0.58 (Tr)<br>3.42 (Te1)<br>3.10 (Te2)<br>2.31 (Te3)<br>2.40 (Te4)<br>1.93 (Te5)<br>1.89 (Te6) | 0.58 (Tr)<br>3.42 (Te1)<br>3.10 (Te2)<br>2.31 (Te3)<br>2.40 (Te4)<br>1.93 (Te5)<br>1.89 (Te6) | 0.66 (Tr)<br>17.06 (Te1)<br>15.57 (Te2)<br>9.30 (Te3)<br>11.95 (Te4)<br>5.45 (Te5)<br>5.41 (Te6) | 0.81 (Tr)<br>4.13 (Te1)<br>3.95 (Te2)<br>3.05 (Te3)<br>3.46 (Te4)<br>2.34 (Te5)<br>2.33 (Te6) | 0.56 (Tr)<br>2.32 (Te1)<br>2.44 (Te2)<br>1.99 (Te3)<br>2.49 (Te4)<br>1.32 (Te5)<br>1.36 (Te6) | 0.99 (Tr)<br>0.89 (Te1)<br>0.93 (Te2)<br>0.96 (Te3)<br>0.93 (Te4)<br>0.97 (Te5)<br>0.94 (Te6) |

\*Tr = training and Te = Testing

In order to ensure good ANN model generalization, the developed model must perform well when tested with data that are different from the previously used training data. In the literature [9], [14]–[27], [13], [30]–[34], developed ANN path loss models were tested with data obtained from radio networks that operate at the same signal frequency as that of the training data. In this new study, ANN path loss model was developed using RSS data obtained from VHF network (NTA-BENIN, 189.25 MHz); while the generalization ability of the developed ANN path loss model was tested using six subsets of data collected from UHF network (ITV-BENIN, 479.25 MHz).

Table 3 shows that this new study considered a wider range of parameters for both neural network configuration and model training in terms of input data variables, data heterogeneity, activation functions, number of hidden layer and neurons, learning algorithms, and performance metrics.

As shown in Table 4, this new study employs all the six model performance evaluation metrics (ME, MAE, MSE, RMSE, SD and R) to assess the accuracy and generalization ability of the developed ANN path loss model. This study achieved higher prediction accuracy and better generalization performance than existing models.

Therefore, the summary of the contributions of this paper is the outcome of the extensive experimentations of neural network optimization (as evident in Table 2) that was conducted to determine the optimal network parameters for path loss predictions in VHF band. Field measurement campaigns were conducted in the urban areas of Benin City, Edo State, Nigeria to measure terrain profile data of the receiver and path losses of signal transmitted at 189.25 MHz and 479.25 MHz. Different ANN architectures were trained with varying number of input parameters and hidden neurons. Also, the ANN training was performed based on different learning algorithms and activation functions. At the end of each experimentation, the performance of the model was evaluated using statistical metrics including MAE, MSE, RMSE, SD and R.

### III. MATERIALS AND METHOD

#### A. MEASUREMENT SET-UP AND DATA COLLECTION

An experimental set-up was designed and implemented to measure and record the RSS of the radio signal received from the transmitting antennas of two broadcasting stations located in Benin City, Edo State, Nigeria (i.e. NTA-BENIN and ITV-BENIN). The broadcasting stations transmit radio signals using omnidirectional antennas with power of 10 kW



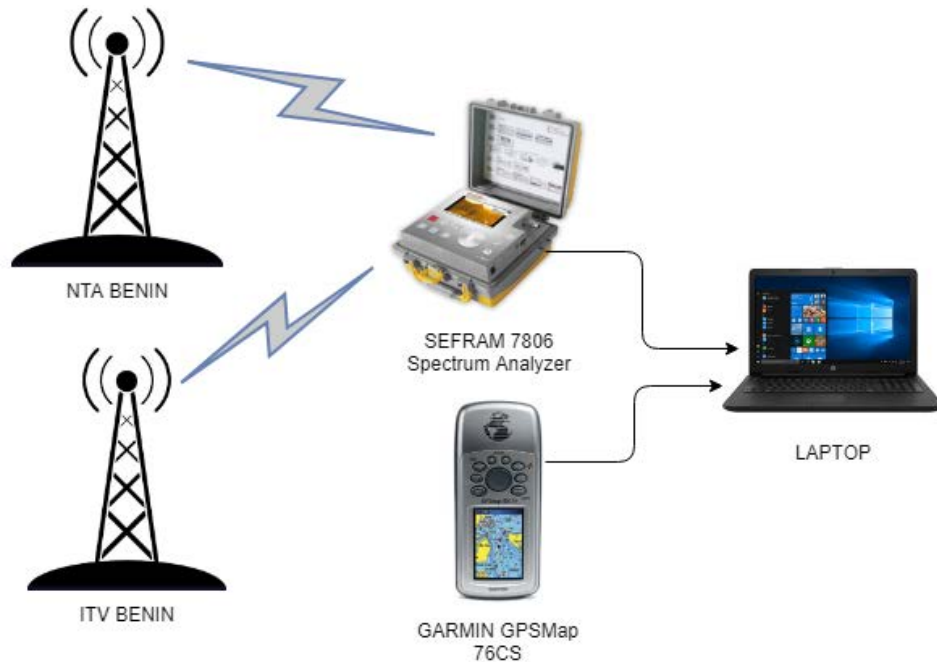


FIGURE 1. RSS measurement set-up.

at 300 metres transmitter height. The measurement set-up consists of a portable spectrum analyser (SEFRAM 7806), a GPS (Global Positioning System) and a personal computer (laptop) as shown in Figure 1.

The spectrum analyzer was used to measure the RSS at different distances from the transmitting antennas. SEFRAM 7806 is a cost-effective measurement instrument used by field technicians and engineers for basic signal investigations, thereby eliminating the need for a full-featured conventional spectrum analyzer. It is suitable for terrestrial analogue and digital television networks. The battery-operated handheld digital meter is equipped with a lithium-ion battery and it is capable of measuring radio frequency signal strength levels with a frequency range of 45-865 MHz.

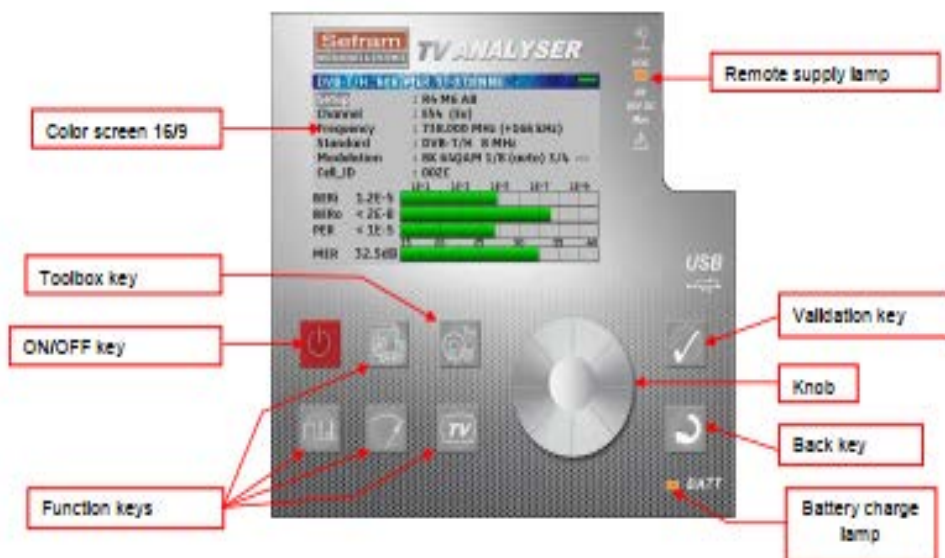
The spectrum analyzer was set-up accordingly: remote supply was set using the toolbox key; received signal was identified using the spectrum key; the parameters of the received signal were adjusted using the measurement key; the signal reception was completely validated using the TV key; the value to be modified was selected using the validation key; and the value was adjusted using the knob key. The functionalities of the keys and a typical display output of SEFRAM 7806 are shown in Figure 2. The resolution of the spectrum analyzer for terrestrial measurement is 50 kHz. In addition, a handheld GPS (GARMIN GPS 76CS) receiver was used to obtain the spatial coordinates of the measuring points in degrees, and to measure the elevation of the receiver's location. SEFRAM 7806 and GARMIN GPS 76CS were connected to a laptop for efficient data logging. The measured RSS data were transferred to the laptop through Universal Serial Bus (USB) interfaces. The path losses between the

transmitting antenna and the receiving antenna were obtained by subtracting the RSS values from the transmitted power.

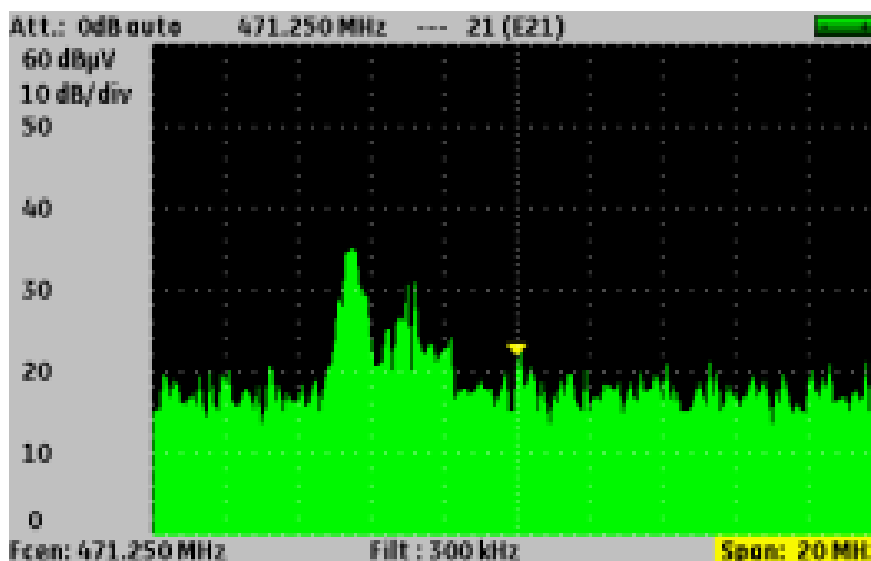
Field measurement campaigns were conducted in the urban areas of Benin, Edo State, Nigeria to obtain relevant geographical and network information. RSS data collected through drive tests were used to quantify the path losses of radio signals transmitted at 189.25 and 479.25 MHz from the antennas of NTA-BENIN and ITV-BENIN broadcasting stations. The study location forms the nucleus of the Niger Delta region in Nigeria. Edo State borders at Kogi State (North), Delta State (East and South), Ekiti and Ondo States (West). The climatic condition is usually tropical, made up of two major seasons including the wet (or rainy) and dry seasons. Six drive test routes were planned and surveyed including: Ekpoma-Auchi, A232, Benin-Warri, Benin-Okumu, Ekenwa, and Sagamu-Benin Expressway roads. Figure 3 shows the digitized map of Edo State, displaying the locations of where measurement samples were taken.

## B. DEVELOPMENT OF ARTIFICIAL NEURAL NETWORK MODEL FOR PATH LOSS PREDICTION

The proposed Feed Forward Neural Network (FFNN) model was developed in accordance with various objectives, which include varying: the number of inputs, number of hidden neurons, activation function and training algorithms. A single hidden layer with suitable number of hidden neurons were used to approximate arbitrary continuous function [35]. Theoretical works and many experimental results have shown that a single hidden layer is sufficient for ANN to approximate any complex nonlinear function. Many researchers in the field of ANN suggest that it is usually unnecessary to



(a)



(b)

**FIGURE 2.** (a) SEFRAM 7806 spectrum analyzer functionalities (b) Sample RSS measurement waveform.

use more than one hidden layer in a multilayer feedforward network. Indeed, many experimental results in other application areas confirmed that one hidden layer is enough to produce high prediction accuracy and good generalization ability for regression problems [36]–[40]. Additional hidden layer may introduce more complexity, thereby increasing training time and memory requirements. It may also lead to model over-fitting, especially when the data size is not sufficiently large.

The obtained measurement data from the drive tests conducted along twelve routes were divided into training and testing datasets. The testing dataset was used to evaluate the generalization ability of the developed ANN models. Therefore, the complete dataset was distributed into 70%

training, 15% validation and 15% testing. In the course of the model development and experimentations, the suitability of three popularly used activation functions was carefully investigated. The mathematical representations of the activation functions are given by equations (1)–(3) respectively [30]:

- i Logistic sigmoid activation function (logsig)

$$f(u) = \frac{1}{1+e^{-u}} \tag{1}$$

- ii Hyperbolic tangent sigmoid activation function (tansig)

$$f(u) = \frac{2}{1+e^{-2u}} \tag{2}$$



FIGURE 3. Map showing RSS measurement routes.

iii Linear activation function (purelin)

$$f(u) = u \quad (3)$$

In addition, the efficiency of the eight training algorithms [41] were examined. The choice of the most appropriate training algorithm for ANN model development usually depends the complexity of the task, training data size, the sizes of the weight and bias vectors, the error target, and area of application. In this study, we investigated the effectiveness of eight training algorithms to justify their

use for path loss predictions. These training algorithms are: (a) Levenberg-Marquardt backpropagation (LM); (b) BFGS quasi-Newton backpropagation (BFGS); (c) Resilient backpropagation (RP); (d) Scaled conjugate gradient backpropagation (SCG); (e) Conjugate gradient backpropagation with Fletcher-Reeves updates (CGF); (f) Conjugate gradient backpropagation with Polak-Ribière updates (CGP); (g) One-step secant backpropagation (OSS); and (h) Gradient descent with momentum and adaptive learning rate backpropagation (GDX).

LM is one of the most commonly used training algorithms for supervised learning owing to its high speed. However, its computation processes are often memory-intensive. The theoretical background and mathematical formulation of LM algorithm are detailed in [42]–[44]. Usually, the training data is randomly divided into three: training, validation and testing data subsets. The training data subset is supported by the validation and validation data subsets. Validation subset is used to achieve early stopping of training process once there is no significant improvement in the network performance while the generalization ability of the neural network is monitored using the testing subset. For any neural network to be trained using LM algorithm, the network weight, net input, and activation functions must be derivable. The major drawback here is the use of average or sum of squared errors as performance metric in Jacobian computations.

SCG algorithm was developed based on conjugate directions with no line search at every iteration [45]. In CGF algorithm, the search for the steepest descent direction begins with the first iteration and the weight and bias are updated based on conjugate gradient backpropagation with Fletcher-Reeves updates. A conjugate search direction is realized by combining both the new and previous steepest descent directions together. Elaborate information about CGF algorithms can be found in [43], [46]. This algorithm requires additional memory space than primitive methods but they are most suitable for networks with large number of weights. CGP is a different conjugate gradient method developed by Polak and Ribière. Here, the weight and bias are updated based on conjugate gradient backpropagation with Polak-Ribière updates [47].

In BFGS algorithm, the weight and bias of the network are updated using BFGS quasi-Newton method described in [48], [49]. For faster convergence during the optimization process, Newton's method was developed to replace conjugate gradient method. However, the replacement comes with complex and memory-intensive computations. Quasi-Newton method eliminated the need for the computation of second derivatives by updating an estimate Hessian matrix at every iteration. BFGS algorithm is an improved quasi-Newton method based on Broyden, Fletcher, Goldfarb, and Shanno update. Although the algorithm converges faster with fewer iterations

when compared to conjugate gradient approach, BFGS performs large computations for every iteration and it requires additional memory space. BFGS algorithm will be most suitable for smaller feedforward neural networks.

RP algorithm employs resilient backpropagation method to mitigate the challenges of partial derivatives introduced by the steepest descent used with sigmoid functions during multilayer network training. The sign of the derivate is determined solely by the direction of the weight update with no regard for the magnitude of the derivative. A different update is used to calculate the magnitude of changes in weight. A detailed description of the RP method is provided in [50]. GDX is a network training function that updates weight and bias values by combining adaptive learning rate with momentum training. GDX can train any network as long as its weight, net input, and transfer functions have derivative functions.

Owing to the need for more memory and computation requirements in BFGS algorithm at every iteration than the conjugate gradient algorithms, there is need for a secant approximation to reduce the demands. OSS algorithm is an attempt to bridge the gap between the conjugate gradient algorithms and the quasi-Newton (secant) algorithms. This algorithm does not store the complete Hessian matrix; it assumes that at each iteration, the previous Hessian was the identity matrix. This has the additional advantage that the new search direction can be calculated without computing a matrix inverse. This algorithm requires less storage and computation per epoch than the BFGS algorithm. It requires slightly more storage and computation per epoch than the conjugate gradient algorithms. It can be considered a compromise between full quasi-Newton algorithms and conjugate gradient algorithms. More information about OSS method can be found in [51].

The performance of the developed ANN models was evaluated based on the following statistical metrics: MAE, MSE, RMSE, SD, and R. The metrics are given by equations (4)–(8), as shown at the bottom of this page, respectively.

The proposed ANN model architecture design and experimentation framework shown in Figure 4 was implemented in MATLAB 2016b to determine the most appropriate network bias and weight values, number of inputs, number of neurons,

$$MAE = \frac{1}{n} \sum_{i=1}^n (PL_i^m - PL_i^p) \quad (4)$$

$$MSE = \frac{1}{n} \sum_{i=1}^n (PL_i^m - PL_i^p)^2 \quad (5)$$

$$RMSE = \sqrt{\frac{1}{n} \sum_{i=1}^n (PL_i^m - PL_i^p)^2} \quad (6)$$

$$SD = \sqrt{\frac{1}{n} \sum_{i=1}^n (|PL_i^m - PL_i^p| - \mu)^2} \quad (7)$$

$$R = \frac{\sum_{i=1}^n (PL_{i,measured} - PL_{measured,mean})^2 - \sum_{i=1}^n (PL_{i,predicted} - PL_{i,measured})^2}{\sum_{i=1}^n (PL_{i,measured} - PL_{measured,mean})^2} \quad (8)$$



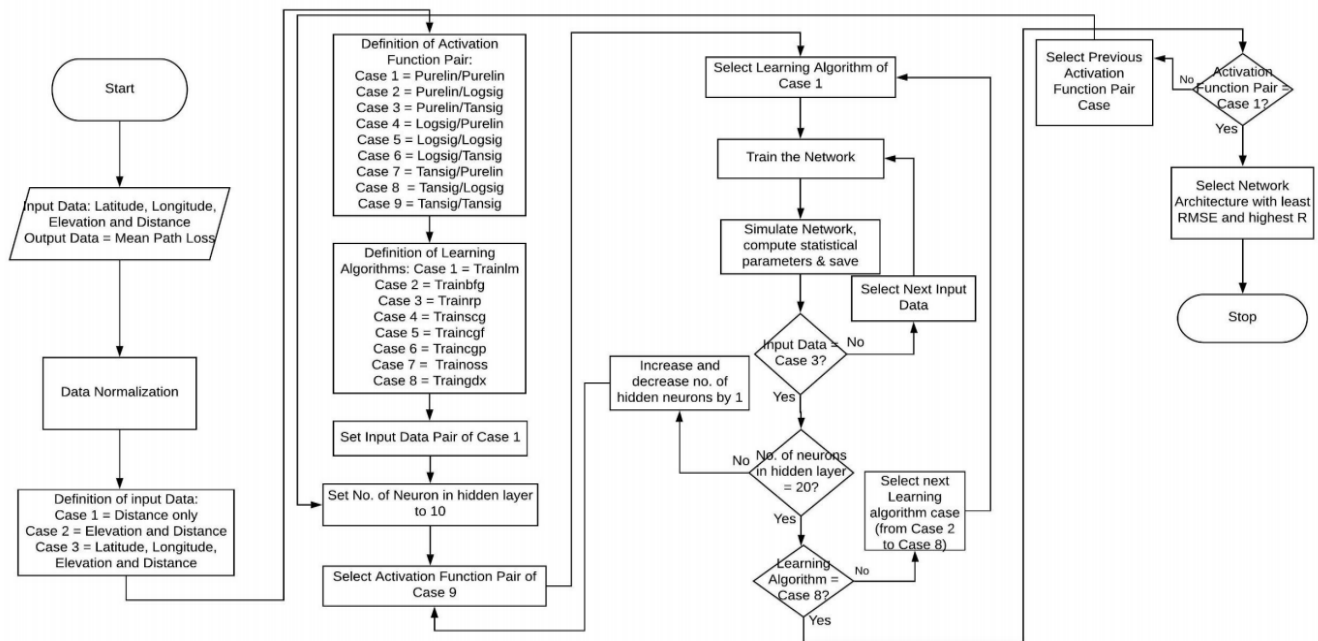


FIGURE 4. Flow chart of ANN model development process.

training algorithm and activation function type to be used in the optimal ANN model development. We investigated the effects of the kind of inputs, number of hidden layer neurons, activation function and training algorithm on the performance of ANN models designed for path loss predictions. The most suitable number of neurons, number of inputs, learning algorithm and activation function pairs were determined through carefully designed extensive experimentations.

IV. RESULTS AND DISCUSSIONS

In this section, the analysis of the data as well as the results of the study are presented and discussed with respect to the aim and objectives of this study. The data obtained from the field measurement campaign were analyzed to verify the validity of the acquired data, and then used for ANN model training, validation and testing. Furthermore, a comparative study of the ANN path loss predictions and those of empirical models (Hata, COST 231, Egli and ECC-33) was performed to ascertain the efficacy of ANN models for path loss prediction.

RSS measurement data collected through drive tests in the urban propagation environments were evaluated along the planned survey routes. The drive tests were conducted along twelve major routes, six each for NTA-BENIN and ITV-BENIN broadcasting stations. The routes include Ekpoma-Auchi Road, A232 Road, Benin-Warri Road, Benin-Okumu Road, Ekenwa Road and Sagamu-Benin Expressway. The number of data instances obtained from each of these routes are presented in Table 5. A total of 285 and 253 data instances were collected over ITV-BENIN and NTA-Benin network respectively.

Table 6 presents the distances covered during the drive tests for each of the routes. ITV-BENIN drive test conducted along

TABLE 5. Data instances collected along 12 drive test routes.

| S/N   | Route                   | Training Data (189.25 MHz) | Testing Data (479.25 MHz) |
|-------|-------------------------|----------------------------|---------------------------|
| 1     | Ekpoma-Auchi Road       | 69                         | 76                        |
| 2     | A232 Road               | 50                         | 62                        |
| 3     | Benin-Warri Road        | 39                         | 48                        |
| 4     | Benin-Okumu Road        | 10                         | 19                        |
| 5     | Ekenwa Road             | 11                         | 20                        |
| 6     | Sagamu-Benin Expressway | 74                         | 60                        |
| Total |                         | 253                        | 285                       |

TABLE 6. Data instances collected along 12 drive test routes.

| S/N | Route                   | Total distance from NTA-BENIN transmitter (km) | Total distance from ITV-BENIN transmitter (km) |
|-----|-------------------------|--|--|
| 1   | Ekpoma-Auchi Road       | 89.59  | 90.26  |
| 2   | A232 Road               | 46.71  | 57.39  |
| 3   | Benin-Warri Road        | 27.68  | 38.11  |
| 4   | Benin-Okumu Road        | 8.71   | 12.32  |
| 5   | Ekenwa Road             | 11.33  | 14.17  |
| 6   | Sagamu-Benin Expressway | 69.06  | 56.61  |

Ekpoma-Auchi road covered a total distance of 90.26 km from the transmitting antenna. Similarly, the total distances covered along A232, Benin-Warri, Benin-Okumu, Ekenwa, and Sagamu-Benin Expressway are 57.39 km, 38.11 km, 12.32 km, 14.17 km and 56.61 km respectively.



**TABLE 7. Statistical description of the training dataset.**

|                    | Latitude | Longitude | Elevation (m) | Distance (km) | Mean Path Loss (dB) |
|--------------------|----------|-----------|---------------|---------------|---------------------|
| Mean               | 6.47     | 5.72      | 38.07         | 30.74         | 152.71              |
| Median             | 6.44     | 5.68      | 30.48         | 25.76         | 153.27              |
| Mode               | 6.36     | 5.67      | 30.78         | 0.49          | 150.60              |
| Standard Deviation | 0.18     | 0.26      | 26.95         | 22.88         | 6.43                |
| Variance           | 0.03     | 0.07      | 726.27        | 523.63        | 41.39               |
| Kurtosis           | 1.99     | 2.52      | 5.18          | 2.45          | 6.88                |
| Skewness           | 0.29     | 0.05      | 1.65          | 0.65          | -1.00               |
| Range              | 0.78     | 1.10      | 118.57        | 89.56         | 41.07               |
| Minimum            | 6.11     | 5.18      | 7.01          | 0.03          | 127.30              |
| Maximum            | 6.89     | 6.27      | 125.58        | 89.59         | 168.37              |

**TABLE 8. Statistical description of the testing sub-dataset (R1).**

|                    | Latitude | Longitude | Elevation (m) | Distance (km) | Mean Path Loss (dB) |
|--------------------|----------|-----------|---------------|---------------|---------------------|
| Mean               | 6.61     | 5.96      | 65.78         | 45.03         | 157.83              |
| Median             | 6.61     | 5.96      | 55.17         | 44.79         | 160.53              |
| Mode               | 6.39     | 6.06      | 49.68         | 61.81         | 153.30              |
| Standard Deviation | 0.15     | 0.20      | 31.42         | 26.29         | 7.28                |
| Variance           | 0.02     | 0.04      | 987.02        | 691.24        | 52.95               |
| Kurtosis           | 1.64     | 1.91      | 1.93          | 1.81          | 4.73                |
| Skewness           | 0.04     | 0.02      | 0.44          | 0.05          | -1.35               |
| Range              | 0.51     | 0.67      | 115.52        | 89.73         | 35.14               |
| Minimum            | 6.39     | 5.61      | 10.06         | 0.53          | 134.03              |
| Maximum            | 6.89     | 6.27      | 125.58        | 90.26         | 169.17              |

The NTA-BENIN drive tests along the same routes covered total distances of 89.59 km, 46.71 km, 27.68 km, 8.71 km, 11.33 km and 69.06 km respectively. RSS data obtained from NTA-BENIN and ITV-BENIN were used for neural network training and testing respectively. The plots of the training data and the testing data are shown in Figures 5 and 6. Regarding open and public accessibility of data for research reproducibility, our aim is to submit a data article for future publication in an open access journal. A similar approach was adopted in our previous research [7], [28], [29].

Tables 7-13 present the statistical description of the training dataset and the testing sub-datasets. The descriptive statistical measures include the: mean, median, mode, standard deviation, variance, kurtosis, skewness, range, minimum and maximum. This depicts the difference between the testing and training datasets and confirms the validity of the generalization ability for the developed ANN model, while presenting an overall summary of the data under consideration.

Tables 14–17 show the path loss prediction values obtained by considering the various cases. In Case I, there is only one

**TABLE 9. Statistical description of the testing sub-dataset (R2).**

|                    | Latitude | Longitude | Elevation (m) | Distance (km) | Mean Path Loss (dB) |
|--------------------|----------|-----------|---------------|---------------|---------------------|
| Mean               | 6.33     | 5.83      | 29.17         | 29.60         | 156.42              |
| Median             | 6.31     | 5.82      | 28.04         | 29.54         | 157.17              |
| Mode               | 6.29     | 5.61      | 24.99         | 1.94          | 157.03              |
| Standard Deviation | 0.06     | 0.14      | 8.48          | 16.27         | 7.68                |
| Variance           | 0.00     | 0.02      | 71.84         | 264.67        | 58.99               |
| Kurtosis           | 3.24     | 1.75      | 3.22          | 1.81          | 4.66                |
| Skewness           | 1.25     | 0.17      | 0.43          | 0.03          | -1.12               |
| Range              | 0.18     | 0.48      | 39.32         | 55.45         | 36.90               |
| Minimum            | 6.28     | 5.61      | 10.36         | 1.94          | 131.40              |
| Maximum            | 6.46     | 6.08      | 49.68         | 57.39         | 168.30              |

**TABLE 10. Statistical description of the testing sub-dataset (R3).**

|                    | Latitude | Longitude | Elevation (m) | Distance (km) | Mean Path Loss (dB) |
|--------------------|----------|-----------|---------------|---------------|---------------------|
| Mean               | 6.29     | 5.65      | 23.06         | 18.07         | 152.69              |
| Median             | 6.32     | 5.63      | 25.30         | 14.94         | 154.43              |
| Mode               | 6.13     | 5.61      | 11.89         | 11.96         | 153.63              |
| Standard Deviation | 0.09     | 0.15      | 9.77          | 10.47         | 8.83                |
| Variance           | 0.01     | 0.02      | 95.47         | 109.72        | 77.93               |
| Kurtosis           | 1.92     | 42.67     | 1.68          | 2.08          | 4.23                |
| Skewness           | -0.39    | 6.35      | 0.15          | 0.29          | -1.10               |
| Range              | 0.33     | 1.14      | 33.83         | 37.75         | 39.07               |
| Minimum            | 6.11     | 5.50      | 9.45          | 0.36          | 127.00              |
| Maximum            | 6.44     | 6.64      | 43.28         | 38.11         | 166.07              |

**TABLE 11. Statistical description of the testing sub-dataset (R4).**

|                    | Latitude | Longitude | Elevation (m) | Distance (km) | Mean Path Loss (dB) |
|--------------------|----------|-----------|---------------|---------------|---------------------|
| Mean               | 6.38     | 5.61      | 33.04         | 7.64          | 145.57              |
| Median             | 6.37     | 5.61      | 32.77         | 9.12          | 147.30              |
| Mode               | 6.34     | 5.59      | 34.14         | 0.36          | 127.00              |
| Standard Deviation | 0.03     | 0.01      | 4.19          | 3.88          | 9.13                |
| Variance           | 0.00     | 0.00      | 17.52         | 15.09         | 83.41               |
| Kurtosis           | 1.99     | 2.52      | 3.24          | 2.07          | 2.62                |
| Skewness           | 0.58     | 0.41      | 0.98          | -0.63         | -0.73               |
| Range              | 0.10     | 0.04      | 15.12         | 11.96         | 32.77               |
| Minimum            | 6.34     | 5.59      | 28.16         | 0.36          | 127.00              |
| Maximum            | 6.44     | 5.63      | 43.28         | 12.32         | 159.77              |

ANN input attribute (i.e. distance). In Case II, there are two ANN input attributes (i.e. distance and elevation). In Case III, there are four ANN input attributes (i.e. longitude, latitude,

TABLE 12. Statistical description of the testing sub-dataset (R5).

|                    | Latitude | Longitude | Elevation (m) | Distance (km) | Mean Path Loss (dB) |
|--------------------|----------|-----------|---------------|---------------|---------------------|
| Mean               | 6.37     | 5.61      | 31.44         | 8.52          | 145.93              |
| Median             | 6.36     | 5.61      | 32.61         | 9.65          | 147.63              |
| Mode               | 6.32     | 5.58      | 34.14         | 0.36          | 127.00              |
| Standard Deviation | 0.04     | 0.01      | 5.80          | 4.51          | 8.91                |
| Variance           | 0.00     | 0.00      | 33.62         | 20.37         | 79.33               |
| Kurtosis           | 1.83     | 2.83      | 2.52          | 1.91          | 2.69                |
| Skewness           | 0.41     | -0.37     | 0.12          | -0.50         | -0.93               |
| Range              | 0.12     | 0.05      | 21.95         | 13.81         | 28.17               |
| Minimum            | 6.32     | 5.58      | 21.34         | 0.36          | 127.00              |
| Maximum            | 6.44     | 5.63      | 43.28         | 14.17         | 155.17              |

TABLE 13. Statistical description of the testing sub-dataset (R6).

|                    | Latitude | Longitude | Elevation (m) | Distance (km) | Mean Path Loss (dB) |
|--------------------|----------|-----------|---------------|---------------|---------------------|
| Mean               | 6.60     | 5.39      | 26.11         | 28.71         | 153.34              |
| Median             | 6.60     | 5.39      | 22.25         | 28.48         | 153.80              |
| Mode               | 6.45     | 5.58      | 11.28         | 0.51          | 160.37              |
| Standard Deviation | 0.08     | 0.13      | 13.38         | 16.56         | 6.04                |
| Variance           | 0.01     | 0.02      | 178.96        | 274.35        | 36.46               |
| Kurtosis           | 2.18     | 1.70      | 1.62          | 1.81          | 5.23                |
| Skewness           | -0.13    | -0.01     | 0.18          | 0.01          | -1.24               |
| Range              | 0.29     | 0.42      | 41.45         | 56.10         | 30.77               |
| Minimum            | 6.45     | 5.18      | 7.01          | 0.51          | 130.90              |
| Maximum            | 6.74     | 5.59      | 48.46         | 56.61         | 161.67              |

distance and elevation). The training dataset was trained using the Levenberg-Marquardt algorithm, with 10 hidden neurons and hyperbolic tangent sigmoid (tansig, tansig) activation function. The performance results of the three input scenarios are presented in Table 14. The experiment indicated that the inclusion of a larger number of inputs produced the least error with MAE, MSE, RMSE, SD and R values of 0.68 dB, 0.89 dB, 0.94 dB, 0.66 dB and 0.98 respectively.

Table 15 represents the values derived as a result of varying the number of hidden neurons from 1 – 20. The dataset was trained using LM algorithm, the hyperbolic tangent sigmoid (tansig, tansig) activation function and the four input instances (latitude, longitude, elevation and distance). Nine hidden neurons recorded the least error with MAE, MSE, RMSE, SD and R values of 0.64 dB, 0.81 dB, 0.90 dB, 0.63 dB and 0.99 respectively.

In Table 16, LM algorithm was employed in training the model, as well as 9 hidden neurons and the four input instances. The logistic sigmoid (logsig), hyperbolic tangent sigmoid (tansig) and the linear (purelin) activation

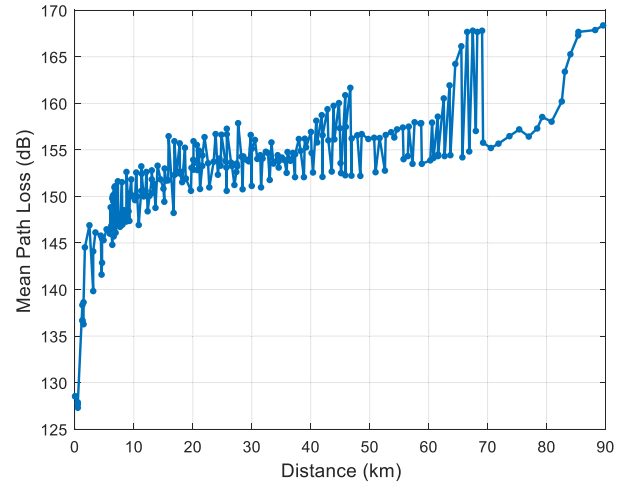


FIGURE 5. Training data collected from VHF Transmitter (189.25 MHz) at varying distances.

TABLE 14. Performance evaluation for varying input variables.

| Case | ME (dB) | MAE (dB) | MSE (dB) | RMSE (dB) | SD (dB) | R      |
|------|---------|----------|----------|-----------|---------|--------|
| I    | 1.8533  | 1.8533   | 5.7434   | 2.3965    | 1.5195  | 0.9280 |
| II   | 1.2490  | 1.2490   | 2.8189   | 1.6790    | 1.1220  | 0.9671 |
| III  | 0.6786  | 0.6786   | 0.8965   | 0.9469    | 0.6604  | 0.9898 |

functions were considered while conducting the experiment. The results retrieved specified that the use of the hyperbolic tangent sigmoid (tansig) activation function at both the hidden and output layer produced the least error with MAE, MSE, RMSE, SD and R values of 0.58 dB, 0.66 dB, 0.81 dB, 0.56 dB and 0.99 respectively.

In Table 17, various training algorithms were considered, while nine hidden neurons, the four-input instances and the tansig, tansig activation function were employed in training the network. The Levenberg-Marquardt algorithm proved to be the most accurate with MAE, MSE, RMSE, SD and R values of 0.58 dB, 0.66 dB, 0.81 dB, 0.56 dB and 0.99 respectively. Recent research findings support the position of this paper on the efficiency of LM algorithm for prediction tasks in different application areas [52]–[55].

Taking all the results acquired from Tables 14–17, it is evident that the optimal ANN path loss model comprises of the following: multiple input, nine hidden neurons, the tansig, tansig activation function, and the Levenberg-Marquardt learning algorithm. Figure 7 displays the network architecture of the optimal ANN model. The training dataset was divided into sub-datasets with 70% for training, 15% for validation and 15% for testing. Hence, the correlation degree between the path loss values predicted by the optimal ANN model and their corresponding target path loss values in the three sub-datasets of the training dataset is depicted in Figure 8. The training, validation and testing sub-datasets possessed R values of 0.9926, 0.9870 and 0.9873 respectively, while the overall R value for the training process is 0.991, indicating

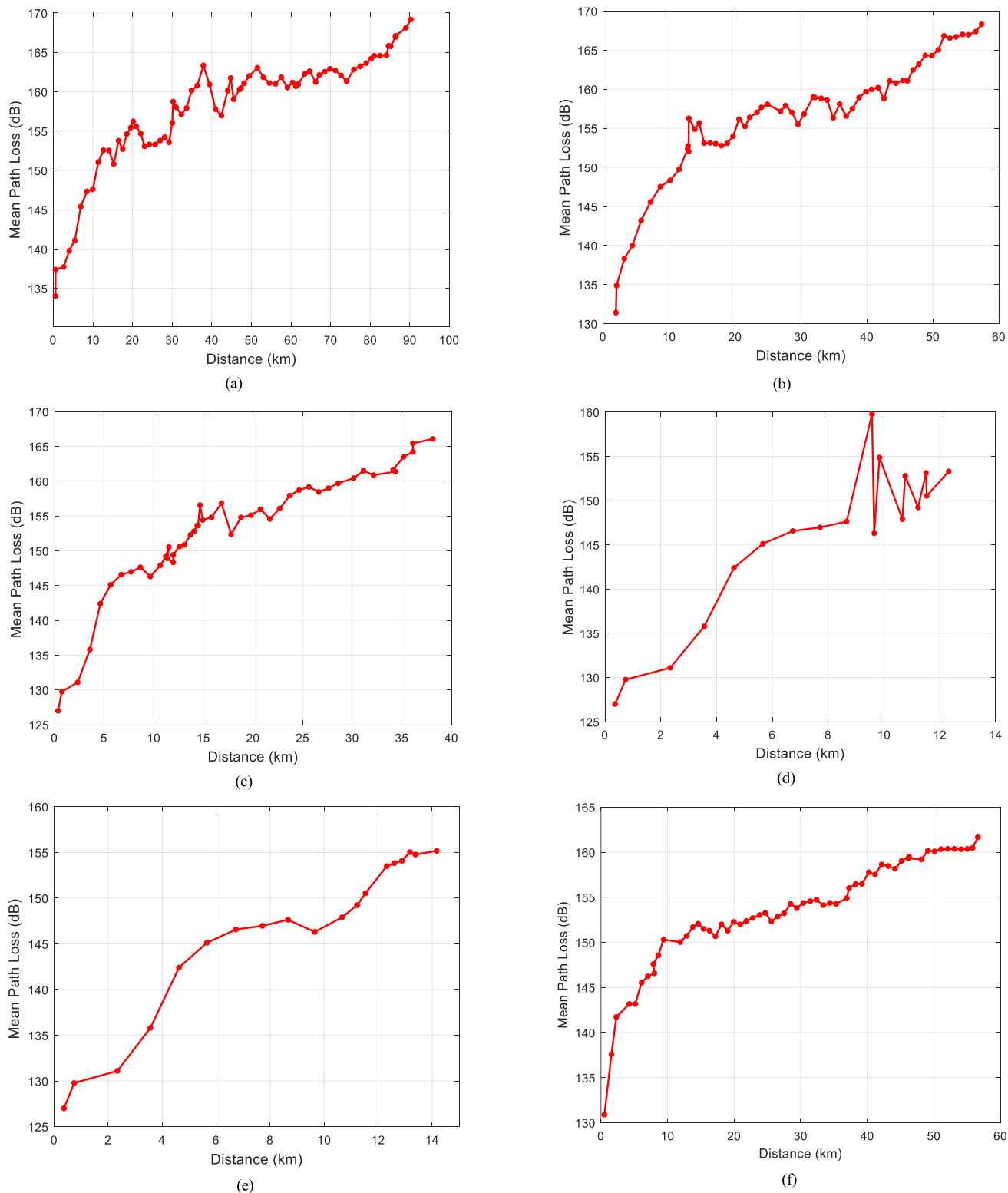


**FIGURE 6.** Testing data collected from UHF Transmitter (479.25 MHz) at varying distances along (a) Route 1 (b) Route 2 (c) Route 3 (d) Route 4 (e) Route 5 (f) Route 6.

that prediction accuracy is guaranteed during radio network planning and optimization.

A comparative analysis of the ANN predicted results and some empirical models (Hata, COST 231, ECC-33 and Egli

models) is presented in Figure 9. It entails the graphical illustration of measured path loss and the predicted path loss values plotted against the distance between the mobile station and the base station transmitter. This was performed to

TABLE 15. Performance evaluation of varying number of hidden neurons.

| Hidden neurons | ME (dB) | MAE (dB) | MSE (dB) | RMSE (dB) | SD (dB) | R      |
|----------------|---------|----------|----------|-----------|---------|--------|
| 1              | 2.2348  | 2.2348   | 10.4937  | 3.2394    | 2.3451  | 0.8671 |
| 2              | 1.3042  | 1.3042   | 3.1381   | 1.7715    | 1.1988  | 0.9614 |
| 3              | 1.1208  | 1.1208   | 1.9823   | 1.4079    | 0.8521  | 0.9758 |
| 4              | 0.8380  | 0.8380   | 1.3864   | 1.1775    | 0.8272  | 0.9830 |
| 5              | 0.8489  | 0.8489   | 1.2807   | 1.1317    | 0.7484  | 0.9846 |
| 6              | 0.7999  | 0.7999   | 1.2623   | 1.1235    | 0.7890  | 0.9846 |
| 7              | 0.7578  | 0.7578   | 1.1448   | 1.0700    | 0.7554  | 0.9861 |
| 8              | 0.7493  | 0.7493   | 1.2590   | 1.1221    | 0.8352  | 0.9847 |
| 9              | 0.6475  | 0.6475   | 0.8183   | 0.9046    | 0.6317  | 0.9901 |
| 10             | 0.7238  | 0.7238   | 1.1158   | 1.0563    | 0.7694  | 0.9865 |
| 11             | 0.9588  | 0.9588   | 1.9377   | 1.3920    | 1.0091  | 0.9770 |
| 12             | 0.6605  | 0.6605   | 3.3595   | 1.8329    | 1.7097  | 0.9611 |
| 13             | 0.8496  | 0.8496   | 1.5102   | 1.2289    | 0.8880  | 0.9820 |
| 14             | 0.8836  | 0.8836   | 1.6576   | 1.2875    | 0.9364  | 0.9798 |
| 15             | 0.8633  | 0.8633   | 1.4984   | 1.2241    | 0.8678  | 0.9839 |
| 16             | 0.6419  | 0.6419   | 1.2559   | 1.1207    | 0.9186  | 0.9852 |
| 17             | 0.6191  | 0.6191   | 1.2332   | 1.1105    | 0.9219  | 0.9854 |
| 18             | 0.5530  | 0.5530   | 1.4648   | 1.2103    | 1.0766  | 0.9824 |
| 19             | 0.9022  | 0.9022   | 1.8495   | 1.3600    | 1.0176  | 0.9773 |
| 20             | 0.7566  | 0.7566   | 1.2130   | 1.1014    | 0.8003  | 0.9852 |

TABLE 16. Performance evaluation of nine pairs of activation function.

| Activation function (hidden layer) | Activation function (output layer) | ME (dB) | MAE (dB) | MSE (dB) | RMSE (dB) | SD (dB) | R     |
|------------------------------------|------------------------------------|---------|----------|----------|-----------|---------|-------|
| purelin                            | purelin                            | 2.122   | 2.122    | 11.345   | 3.368     | 2.616   | 0.852 |
| purelin                            | logsig                             | 2.379   | 2.379    | 16.095   | 4.012     | 3.231   | 0.788 |
| purelin                            | tansig                             | 2.137   | 2.137    | 11.280   | 3.359     | 2.591   | 0.853 |
| logsig                             | purelin                            | 0.706   | 0.706    | 0.923    | 0.961     | 0.651   | 0.989 |
| logsig                             | logsig                             | 1.301   | 1.301    | 11.804   | 3.436     | 3.180   | 0.869 |
| logsig                             | tansig                             | 0.799   | 0.799    | 1.449    | 1.204     | 0.900   | 0.984 |
| tansig                             | purelin                            | 0.739   | 0.739    | 1.098    | 1.048     | 0.743   | 0.987 |
| tansig                             | logsig                             | 1.289   | 1.289    | 11.766   | 3.430     | 3.179   | 0.869 |
| tansig                             | tansig                             | 0.584   | 0.584    | 0.663    | 0.814     | 0.568   | 0.992 |

confirm the validity of the ANN model as the optimal model for path loss prediction, as compared to empirical the models with the aid of the training dataset. It was detected that the four empirical models possessed a similar behavior, although there was an over- and under-prediction of the path loss by the ECC-33 and Egli models respectively. However, the obtained ANN results proved to be more accurate as it depicts a greater resemblance of the measured data.

To evaluate the generalization ability of the model, the testing dataset, comprising of six sub-datasets (consisting of routes 1 to 6), was processed using the ANN network architecture produced during the training process. In order to carry out this experiment, the number of inputs to the model was considered to determine the effect of smaller or larger number of inputs in producing the least error. As shown

TABLE 17. Performance evaluation of varying learning algorithms.

| Learning algorithm | ME (dB) | MAE (dB) | MSE (dB) | RMSE (dB) | SD (dB) | R      |
|--------------------|---------|----------|----------|-----------|---------|--------|
| LM                 | 0.5840  | 0.5840   | 0.6631   | 0.8143    | 0.5675  | 0.9920 |
| BFGS               | 0.8613  | 0.8613   | 1.3705   | 1.1707    | 0.7929  | 0.9836 |
| RP                 | 1.1533  | 1.1533   | 3.2193   | 1.7942    | 1.3745  | 0.9612 |
| SCG                | 0.9316  | 0.9316   | 1.6784   | 1.2955    | 0.9003  | 0.9794 |
| CGF                | 0.8944  | 0.8944   | 1.5486   | 1.2444    | 0.8652  | 0.9811 |
| CGP                | 1.1064  | 1.1064   | 2.5937   | 1.6105    | 1.1703  | 0.9684 |
| OSS                | 0.9071  | 0.9071   | 1.6738   | 1.2938    | 0.9225  | 0.9797 |
| GDX                | 5.7559  | 5.7559   | 57.6165  | 7.5906    | 4.9484  | 0.7072 |

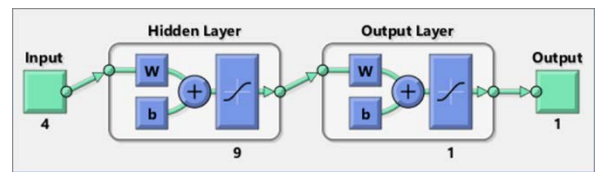


FIGURE 7. Optimal ANN model architecture.

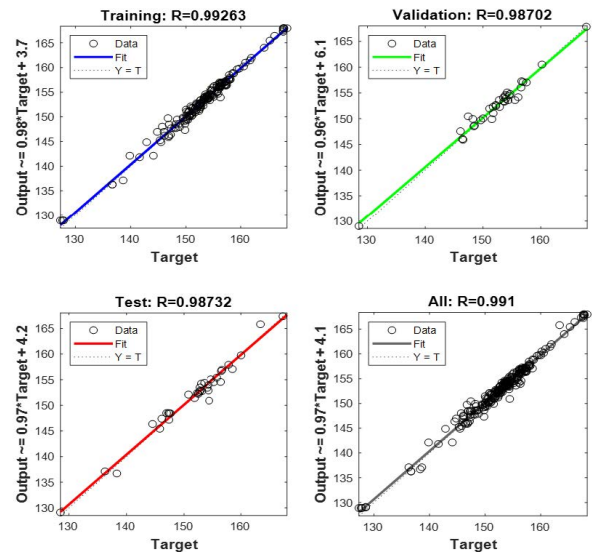


FIGURE 8. R values for optimal ANN model training and validation.

in Figures 10 (a) – (f) and Tables 18 (a) – (f), the results attained proved that the model possesses a good generalization ability, with “neither too little or too large” inputs. Introducing elevation and distance into the model for testing produced the highest regression coefficient, R when compared to the introduction of “Distance only” and “Latitude, Longitude, Elevation and Distance” into the model.

Table 18 (a) depicts the predicted path loss values for the first testing sub-dataset (route 1). It shows that the multiple input parameter produced the best generalization ability with R value of 0.91. Its corresponding graphical representation as displayed in Figure 10 (a) shows an analysis of the

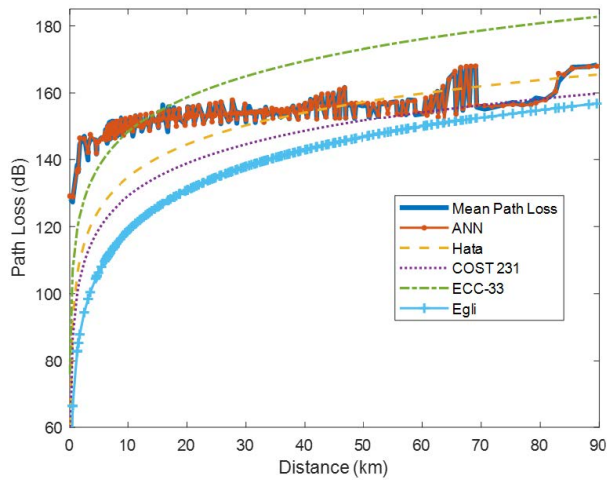


FIGURE 9. Path loss predictions of ANN and empirical models on training data.

generalization ability of the ANN model when subjected to data newly introduced to the model, while taking the number of inputs into consideration. The mean and predicted path loss values were plotted against the distance between the mobile station and the base station transmitter. It was observed that the three instances possessed a somewhat similar behavior, each underestimating the mean path loss. However, the “Latitude, Longitude, Elevation and Distance” criteria presented the greatest resemblance with the mean path loss, while the “Elevation and Distance” criteria illustrated great inaccuracy due to its large deviation from the measured data within the 80 – 90 km range.

The results of the performance evaluation of the second testing sub-dataset (route 2) are presented in Table 18 (b). In this case, the “Distance only” attribute produced the highest regression coefficient value of 0.95, while the least R value of 0.88 was generated by the “Latitude, Longitude, Elevation and Distance” attribute. From the illustration in Figure 10 (b), it is evident that the “Distance only” and the “Elevation and Distance” attributes show similar behavior with the mean path loss while the “Latitude, Longitude, Elevation and Distance” attribute completely underestimates and outliers the measured path loss.

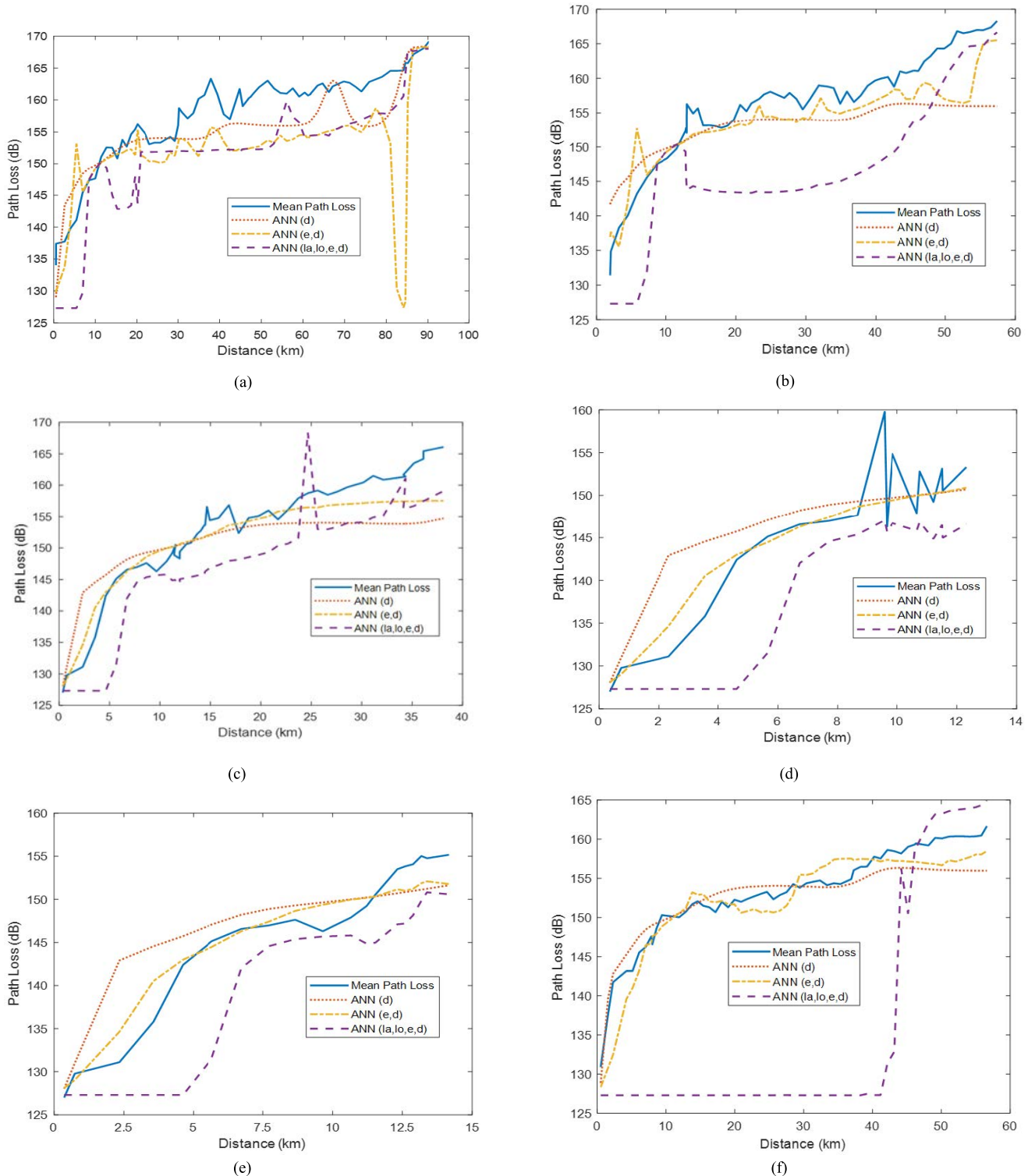
Table 18 (c) portrays a rather different performance evaluation, as the “Elevation and Distance” criteria possesses the highest regression coefficient and the least RMSE value of 0.96 and 3.05 dB respectively as opposed to the “Distance only” attribute with least R value of 0.89. The diagram in Figure 10 (c) proves these estimations, as it depicts the relative closeness of the “Elevation and Distance” attribute to the mean path loss, although a resemblance between both patterns is non-existent. In addition, the “Latitude, Longitude, Elevation and Distance” criteria tend to underestimate the mean path loss entirely, except at the distance range of 24–26 km where it performs over-prediction. This behavior can be attributed to environmental constraints such as presence of clutter, reflection, diffraction, scattering, etc.

TABLE 18. (a) Path loss predictions on testing sub-dataset (R1). (b) Path loss predictions on testing sub-dataset (R2). (c) Path loss predictions on testing sub-dataset (R3). (d) Path loss predictions on testing sub-dataset (R4). (e) Path loss predictions on testing sub-dataset (R5). (f) Path loss predictions on testing sub-dataset (R6).

| (a)  |         |          |          |           |         |        |
|------|---------|----------|----------|-----------|---------|--------|
| Case | ME (dB) | MAE (dB) | MSE (dB) | RMSE (dB) | SD (dB) | R      |
| I    | 3.4160  | 3.4160   | 17.0561  | 4.1299    | 2.3210  | 0.8886 |
| II   | 6.3793  | 6.3793   | 86.4622  | 9.2985    | 6.7651  | 0.5450 |
| III  | 6.1032  | 6.1032   | 49.2697  | 7.0192    | 3.4672  | 0.9176 |
| (b)  |         |          |          |           |         |        |
| Case | ME (dB) | MAE (dB) | MSE (dB) | RMSE (dB) | SD (dB) | R      |
| I    | 4.5228  | 4.5228   | 30.7627  | 5.5464    | 3.2104  | 0.9488 |
| II   | 3.0978  | 3.0978   | 15.5692  | 3.9458    | 2.4439  | 0.9299 |
| III  | 9.2351  | 9.2351   | 104.1382 | 10.2048   | 4.3419  | 0.8838 |
| (c)  |         |          |          |           |         |        |
| Case | ME (dB) | MAE (dB) | MSE (dB) | RMSE (dB) | SD (dB) | R      |
| I    | 3.8388  | 3.8388   | 25.4430  | 5.0441    | 3.2721  | 0.8949 |
| II   | 2.3135  | 2.3135   | 9.3009   | 3.0497    | 1.9871  | 0.9644 |
| III  | 5.8832  | 5.8832   | 42.7254  | 6.5365    | 2.8484  | 0.9190 |
| (d)  |         |          |          |           |         |        |
| Case | ME (dB) | MAE (dB) | MSE (dB) | RMSE (dB) | SD (dB) | R      |
| I    | 3.5212  | 3.5212   | 22.8474  | 4.7799    | 3.2324  | 0.8604 |
| II   | 2.4023  | 2.4023   | 11.9485  | 3.4567    | 2.4855  | 0.9310 |
| III  | 5.8787  | 5.8787   | 52.5131  | 7.2466    | 4.2373  | 0.8785 |
| (e)  |         |          |          |           |         |        |
| Case | ME (dB) | MAE (dB) | MSE (dB) | RMSE (dB) | SD (dB) | R      |
| I    | 3.1466  | 3.1466   | 17.1560  | 4.1420    | 2.6935  | 0.9004 |
| II   | 1.9276  | 1.9276   | 5.4509   | 2.3347    | 1.3173  | 0.9704 |
| III  | 5.1729  | 5.1729   | 40.8078  | 6.3881    | 3.7482  | 0.9081 |
| (f)  |         |          |          |           |         |        |
| Case | ME (dB) | MAE (dB) | MSE (dB) | RMSE (dB) | SD (dB) | R      |
| I    | 1.8859  | 1.8859   | 5.4080   | 2.3255    | 1.3607  | 0.9412 |
| II   | 1.9447  | 1.9447   | 5.9796   | 2.4453    | 1.4824  | 0.9431 |
| III  | 18.8877 | 18.8877  | 454.1835 | 21.3116   | 9.8711  | 0.6307 |

In Table 18(d), the acquired results show a similarity to those obtained in Table 18(c), as “Elevation and Distance” attribute yields the most accurate results, with R value of 0.93, rendering the “Distance only” attribute as the least efficient of the three because to its low regression coefficient of 0.86. The graphical illustration in Figure 10 (d) shows the behavioral patterns of the inputs with respect to the mean path loss. The dissimilarity between the “Distance only” attribute and the measured path loss is apparent, while the “Latitude, Longitude, Elevation and Distance” attribute shows a similar behavior in spite of its underestimation of the model. However, the “Elevation and Distance” attribute depicts a close





**FIGURE 10.** (a) Generalization performance of testing sub-dataset (R1). (b) Generalization performance of testing sub-dataset (R2). (c) Generalization performance of testing sub-dataset (R3). (d) Generalization performance of testing sub-dataset (R4). (e) Generalization performance of testing sub-dataset (R5). (f) Generalization performance of testing sub-dataset (R6).

relation to the mean path loss, proving its ability to achieve good generalization performance.

The results in Table 18(e) and its corresponding illustration in Figure 10 (e) depicts the same outcomes with the

previous and latter experiments (routes 3 and 4). The “Elevation and Distance” input parameter still upholds its efficiency by yielding the highest regression coefficient and the least RMSE of 0.97 and 0.90 respectively. These prediction

values are portrayed in the graphical representation, where the “Distance only” parameter retains a dissimilar pattern to the mean path loss while over-predicting the model. Furthermore, the “Latitude, Longitude, Elevation and Distance” attribute completely under-predicts the model, although it possesses a similar pattern as the measured path loss.

Table 18 (f) exposes the predicted path loss values obtained from the sixth testing sub-dataset (route 6). The highest regression coefficient of 0.94 produced by the “Elevation and Distance” attribute is portrayed in Figure 10 (f), as it depicts the best resemblance to the mean path loss. However, the “Latitude, Longitude, Elevation and Distance” criteria can be described as the outlier in this case as it totally under-predicts the model, except at the 45 – 55km distance range where it performs over-prediction of the measured path loss.

From the obtained results and graphical illustrations presented, the ANN model proved to possess a good generalization ability, with R values of 0.8 and above for the six testing sub-datasets. However, the “Elevation and Distance” attribute produced the highest R values and least RMSE values in most cases, taking instances not initially introduced in the training process into consideration. As earlier stated, the determination of the optimal ANN model was based on some statistical parameters namely: MAE, MSE, RMSE, Standard Deviation and R, in which the predicted path loss values were compared with the target path loss values in both the training and testing datasets. The results obtained from the experiments showed that the network architecture employing all inputs (latitude, longitude, elevation and distance), nine hidden neurons, hyperbolic tangent sigmoid (tansig) activation function and the Levenberg-Marquardt algorithm had the best performance. The FFNN architecture produced the least prediction error with MAE, MSE, RMSE, Standard Deviation and R values of 0.58 dB, 0.66 dB, 0.81 dB, 0.56 dB and 0.99 respectively.

## V. CONCLUSION

In order to design efficient wireless communication systems, the propagation factors of the radio channel often pose serious challenges to radio network engineers whose responsibility is to ensure that subscribers are provided with high speed Internet services at optimum received signal strength. For such efficient network design to be achieved, accurate and reliable path loss models are highly essential for radio network coverage and signal interference predictions.

ANN models have proven to be easier to deploy than deterministic models and they are also more accurate than empirical models. In addition, ANN can be adapted for path loss predictions in rural, suburban and urban propagation environments. Basically, path loss prediction is classified as a regression problem. In this case, ANN model is trained with field measured data to understand the non-linear relationship between the output variable (path loss) and the dependent/input variables such as the frequency of transmission, building height, receiver antenna height, transmitter

antenna height, separation distance between the base station and the mobile station etc. Determination of the appropriate input/feature vector and the correct setting of neural network parameters needed for optimal path loss prediction is very crucial.

In this paper, we conducted an extensive investigation to determine the optimal neural network parameters for path loss prediction in VHF band. Field measurements were conducted in an urban propagation environment to obtain relevant geographical and network information about the receiving mobile equipment and quantify the path losses of radio signals transmitted at 92.3 MHz and 189.25 MHz. Different neural network architectures were trained with varying kinds of input parameters, number of hidden neurons, activation functions, and learning algorithms to accurately predict corresponding path loss values. At the end of the experimentations, the results obtained showed that the ANN model that yielded the best performance employed four input variables (latitude, longitude, elevation, and distance), nine hidden neurons, hyperbolic tangent sigmoid (tansig) activation function, and the Levenberg-Marquardt (LM) learning algorithm with MAE, MSE, RMSE, SD and R values of 0.58 dB, 0.66 dB, 0.81 dB, 0.56 dB and 0.99 respectively. Finally, a comparative analysis of the developed model with Hata, COST 231, ECC-33 and Egli models showed that ANN-based path loss model has better prediction accuracy and generalization ability than the empirical models.

## REFERENCES

- [1] Y. Xing and T. S. Rappaport, “Propagation measurement system and approach at 140 GHz-moving to 6G and above 100 GHz,” in *Proc. IEEE Global Commun. Conf. (GLOBECOM)*, Dec. 2018, pp. 1–6.
- [2] J. Wu, S. Guo, H. Huang, W. Liu, and Y. Xiang, “Information and communications technologies for sustainable development goals: State-of-the-art, needs and perspectives,” *IEEE Commun. Surveys Tuts.*, vol. 20, no. 3, pp. 2389–2406, 3rd Quart., 2018.
- [3] H. L. Bertoni, “Path loss prediction models in cellular communication channels,” in *Wiley Encyclopedia of Telecommunications*. Hoboken, NJ, USA: Wiley, 2003.
- [4] A. R. Mishra, *Advanced Cellular Network Planning and Optimisation: 2G/2.5G/3G... Evolution to 4G*. Hoboken, NJ, USA: Wiley, 2007.
- [5] O. F. Oseni, S. I. Popoola, H. Enumah and A. Gordian, “Radio frequency optimization of mobile networks in Abeokuta, Nigeria for improved quality of service,” *Int. J. Res. Eng. Technol.*, vol. 3, no. 8, pp. 174–180, 2014.
- [6] A. Obot, O. Simeon, and J. Afolayan, “Comparative analysis of path loss prediction models for urban macrocellular environments,” *Nigerian J. Technol.*, vol. 30, no. 3, pp. 50–59, 2011.
- [7] S. I. Popoola, A. A. Atayero, and O. A. Popoola, “Comparative assessment of data obtained using empirical models for path loss predictions in a university campus environment,” *Data Brief*, vol. 18, pp. 380–393, Jun. 2018.
- [8] N. Faruk, S. I. Popoola, N. T. Surajudeen-Bakinde, A. A. Oloyede, A. Abdulkarim, M. Ali, C. T. Calafate, A. A. Atayero, and L. A. Olawoyin, “Path loss predictions in the VHF and UHF bands within urban environments: Experimental investigation of empirical, heuristics and geospatial models,” *IEEE Access*, vol. 7, pp. 77293–77307, 2019.
- [9] S. I. Popoola, E. Adetiba, A. A. Atayero, N. Faruk, C. Yuen, and C. T. Calafate, “Optimal model for path loss predictions using feed-forward neural networks,” *Cogent Eng.*, vol. 5, no. 1, 2018, Art. no. 1444345.
- [10] M. A. Salman, S. I. Popoola, N. Faruk, N. T. Surajudeen-Bakinde, A. A. Oloyede, and L. A. Olawoyin, “Adaptive neuro-fuzzy model for path loss prediction in the VHF band,” in *Proc. Int. Conf. Comput. Netw. Inform. (ICCN)*, Oct. 2017, pp. 1–6.

- [11] N. T. Surajudeen-Bakinde, N. Faruk, S. I. Popoola, M. A. Salman, A. A. Oloyede, and L. A. Olawoyin, "Path loss predictions for multi-transmitter radio propagation in VHF bands using adaptive neuro-fuzzy inference system," *Eng. Sci. Technol., Int. J.*, vol. 21, no. 4, pp. 679–691, Aug. 2018.
- [12] S. I. Popoola, S. Misra, and A. A. Atayero, "Outdoor path loss predictions based on extreme learning machine," *Wireless Pers. Commun.*, vol. 99, no. 1, pp. 441–460, Mar. 2018.
- [13] T. A. Benmus, R. Abboud, and M. K. Shatter, "Neural network approach to model the propagation path loss for great Tripoli area at 900, 1800, and 2100 MHz bands," in *Proc. 16th Int. Conf. Sci. Techn. Autom. Control Comput. Eng. (STA)*, 2015, pp. 793–798.
- [14] E. Ostlin, H.-J. Zepernick, and H. Suzuki, "Macrocell path-loss prediction using artificial neural networks," *IEEE Trans. Veh. Technol.*, vol. 59, no. 6, pp. 2735–2747, Jul. 2010.
- [15] M. Piacentini and F. Rinaldi, "Path loss prediction in urban environment using learning machines and dimensionality reduction techniques," *Comput. Manage. Sci.*, vol. 8, no. 4, pp. 371–385, 2011.
- [16] J. O. Eichie, O. D. Oyedum, M. O. Ajewole, and A. M. Aibinu, "Comparative analysis of basic models and artificial neural network based model for path loss prediction," *Prog. Electromagn. Res. M*, vol. 61, pp. 133–146, 2017. doi: 10.2528/PIERM17060601.
- [17] I. Popescu, I. Nafornita, and P. Constantinou, "Comparison of neural network models for path loss prediction," in *Proc. IEEE Int. Conf. Wireless And Mobile Comput., Netw. Commun. (WiMob)*, Aug. 2005, pp. 44–49.
- [18] G. Cerri, M. Cinalli, F. Michetti, and P. Russo, "Feed forward neural networks for path loss prediction in urban environment," *IEEE Trans. Antennas Propag.*, vol. 52, no. 11, pp. 3137–3139, Nov. 2004.
- [19] S. P. Sotiroudis and K. Siakavara, "Mobile radio propagation path loss prediction using artificial neural networks with optimal input information for urban environments," *AEU-Int. J. Electron. Commun.*, vol. 69, no. 10, pp. 1453–1463, Oct. 2015.
- [20] S. P. Sotiroudis, S. K. Goudos, K. A. Gotsis, K. Siakavara, and J. N. Sahalos, "Application of a composite differential evolution algorithm in optimal neural network design for propagation path-loss prediction in mobile communication systems," *IEEE Antennas Wireless Propag. Lett.*, vol. 12, pp. 364–367, 2013.
- [21] M. Kalakh, N. Kandil, and N. Hakem, "Neural networks model of an UWB channel path loss in a mine environment," in *Proc. IEEE 75th Veh. Technol. Conf. (VTC Spring)*, May 2012, pp. 1–5.
- [22] I. Popescu, I. Nafornita, P. Constantinou, A. Kanatas, and N. Moraitis, "Neural networks applications for the prediction of propagation path loss in urban environments," in *Proc. IEEE VTS 53rd Veh. Technol. Conf. (VTC Spring)*, May 2001, pp. 387–391.
- [23] J. Liu, X. Jin, F. Dong, L. He, and H. Liu, "Fading channel modelling using single-hidden layer feedforward neural networks," *Multidimensional Syst. Signal Process.*, vol. 28, no. 3, pp. 885–903, Jul. 2017.
- [24] N. Zaarour, N. Kandil, N. Hakem, and C. Despins, "Comparative experimental study on modeling the path loss of an UWB channel in a mine environment using MLP and RBF neural networks," in *Proc. Int. Conf. Wireless Commun. Unusual Confined Areas (ICWCUCA)*, 2012, pp. 1–6.
- [25] I. F. Anitzine, J. A. R. Argota, and F. P. Fontán, "Influence of training set selection in artificial neural network-based propagation path loss predictions," *Int. J. Antennas Propag.*, vol. 2012, Oct. 2012, Art. no. 351487.
- [26] A. Ben Zineb and M. Ayadi, "A multi-wall and multi-frequency indoor path loss prediction model using artificial neural networks," *Arabian J. Sci. Eng.*, vol. 41, no. 3, pp. 987–996, 2016.
- [27] P. Gómez-Pérez, M. Crego-García, I. Cuiñas, and R. F. S. Caldeirinha, "Modeling and inferring the attenuation induced by vegetation barriers at 2G/3G/4G cellular bands using artificial neural networks," *Measurement*, vol. 98, pp. 262–275, Feb. 2017.
- [28] S. I. Popoola, A. A. Atayero, O. D. Arausi, and V. O. Matthews, "Path loss dataset for modeling radio wave propagation in smart campus environment," *Data Brief*, vol. 17, pp. 1062–1073, Apr. 2018.
- [29] S. I. Popoola, A. A. Atayero, and N. Faruk, "Received signal strength and local terrain profile data for radio network planning and optimization at GSM frequency bands," *Data Brief*, vol. 16, pp. 972–981, Feb. 2018.
- [30] J. O. Eichie, O. D. Oyedum, M. O. Ajewole, and A. M. Aibinu, "Artificial neural network model for the determination of GSM rxlevel from atmospheric parameters," *Eng. Sci. Technol., Int. J.*, vol. 20, no. 2, pp. 795–804, Apr. 2017.
- [31] A. Bhuvaneshwari, R. Hemalatha, and T. Satyasavithri, "Performance evaluation of dynamic neural networks for mobile radio path loss prediction," in *Proc. IEEE Uttar Pradesh Sect. Int. Conf. Elect., Comput. Electron. Eng. (UPCON)*, Dec. 2016, pp. 461–466.
- [32] J. C. D. Angeles and E. P. Dadios, "Neural network-based path loss prediction for digital TV macrocells," in *Proc. Int. Conf. Humanoid, Nanotechnology, Inf. Technol., Commun. Control, Environ. Manage. (HNICEM)*, 2015, pp. 1–9.
- [33] G. P. Ferreira, L. J. Matos, and J. M. M. Silva, "Improvement of outdoor signal strength prediction in UHF band by artificial neural network," *IEEE Trans. Antennas Propag.*, vol. 64, no. 12, pp. 5404–5410, Dec. 2016.
- [34] M. Ayadi, A. B. Zineb, and S. Tabbane, "A UHF path loss model using learning machine for heterogeneous networks," *IEEE Trans. Antennas Propag.*, vol. 65, no. 7, pp. 3675–3683, Jul. 2017.
- [35] S. Haykin, *Neural Networks: A Comprehensive Foundation*. Upper Saddle River, NJ, USA: Prentice-Hall, 1994.
- [36] R. Noori, A. Khakpour, B. Omidvar, and A. Farokhnia, "Comparison of ANN and principal component analysis-multivariate linear regression models for predicting the river flow based on developed discrepancy ratio statistic," *Expert Syst. Appl.*, vol. 37, no. 8, pp. 5856–5862, Aug. 2010.
- [37] R. Noori, A. R. Karbassi, H. Mehdizadeh, M. Vesali-Naseh, and M. S. Sabahi, "A framework development for predicting the longitudinal dispersion coefficient in natural streams using an artificial neural network," *Environ. Prog. Sustain. Energy*, vol. 30, no. 3, pp. 439–449, Oct. 2011.
- [38] S. Ma, L. Tong, F. Ye, J. Xiao, P. Bénard, and R. Chahine, "Hydrogen purification layered bed optimization based on artificial neural network prediction of breakthrough curves," *Int. J. Hydrogen Energy*, vol. 44, no. 11, pp. 5324–5333, Feb. 2019.
- [39] Y. S. Kong, S. Abdullah, D. Schramm, M. Z. Omar, and S. M. Haris, "Optimization of spring fatigue life prediction model for vehicle ride using hybrid multi-layer perceptron artificial neural networks," *Mech. Syst. Signal Process.*, vol. 122, pp. 597–621, May 2019.
- [40] C. R. Rekha, V. U. Nayar, and K. G. Gopchandran, "Prediction of plasmons in silver nanorods using artificial neural networks with back propagation algorithm," *Optik*, vol. 172, pp. 721–729, Nov. 2018.
- [41] B. Sharma and K. Venugopalan, "Comparison of neural network training functions for hematoma classification in brain CT images," *IOSR J. Comput. Eng.*, vol. 16, no. 1, pp. 31–35, 2014.
- [42] M. T. Hagan and M. B. Menhaj, "Training feedforward networks with the Marquardt algorithm," *IEEE Trans. Neural Netw.*, vol. 5, no. 6, pp. 989–993, Nov. 1994.
- [43] H. B. Demuth, M. H. Beale, O. De Jess, and M. T. Hagan, *Neural Network Design*. Stillwater, OK, USA: Oklahoma State University, 2014.
- [44] D. W. Marquardt, "An algorithm for least-squares estimation of nonlinear parameters," *J. Soc. Ind. Appl. Math.*, vol. 11, no. 2, pp. 431–441, 1963.
- [45] M. F. Møller, "A scaled conjugate gradient algorithm for fast supervised learning," *Neural Netw.*, vol. 6, no. 4, pp. 525–533, Nov. 1993.
- [46] R. Fletcher and C. M. Reeves, "Function minimization by conjugate gradients," *Comput. J.*, vol. 7, no. 2, pp. 149–154, 1964.
- [47] V. K. Gupta, H. Khani, B. Ahmadi-Roudi, S. Mirakhorli, E. Fereyduni, and S. Agarwal, "Prediction of capillary gas chromatographic retention times of fatty acid methyl esters in human blood using MLR, PLS and back-propagation artificial neural networks," *Talanta*, vol. 83, pp. 1014–1022, 2011.
- [48] J. E. Dennis, Jr., and R. B. Schnabel, *Numerical Methods for Unconstrained Optimization and Nonlinear Equations* vol. 16. Philadelphia, PA, USA: SIAM, 1996.
- [49] P. E. Gill, W. Murray, and M. H. Wright, *Practical Optimization*. London, U.K.: Academic, 1981.
- [50] M. Riedmiller and H. Braun, "A direct adaptive method for faster back-propagation learning: The RPROP algorithm," in *Proc. IEEE Int. Conf. Neural Netw.*, Mar. 1993, pp. 586–591.
- [51] R. Battiti, "First- and second-order methods for learning: Between steepest descent and Newton's method," *Neural Comput.*, vol. 4, pp. 141–166, Mar. 1992.
- [52] S. Sadeghi-Esfahlani, J. Butt, and H. Shirvani, "Fusion of artificial intelligence in neuro-rehabilitation video games," *IEEE Access*, vol. 7, pp. 102617–102627, 2019.
- [53] B. Lv, Y. Chen, H. Dai, S. Su, and M. Lin, "PKBPNN-based tracking range extending approach for TMR magnetic tracking system," *IEEE Access*, vol. 7, pp. 63123–63132, 2019.



- [54] A. Garcés-Jimenez, J. L. Castillo-Sequera, A. Del Corte-Valiente, J. M. Gómez-Pulido, and E. P. D. González-Seco, "Analysis of artificial neural network architectures for modeling smart lighting systems for energy savings," *IEEE Access*, vol. 7, pp. 119881–119891, 2019.
- [55] Q. Yao, H. Yang, R. Zhu, A. Yu, W. Bai, Y. Tan, J. Zhang, and H. Xiao, "Core, mode, and spectrum assignment based on machine learning in space division multiplexing elastic optical networks," *IEEE Access*, vol. 6, pp. 15898–15907, 2018.



**SEGUN I. POPOOLA** received the B.Tech. degree (Hons.) in electronic and electrical engineering from the Ladoké Akintola University of Technology, Ogbomoso, Nigeria, and the M.Eng. degree in information and communication engineering from the Department of Electrical and Information Engineering, Covenant University, Ota, Nigeria. He is currently pursuing the Ph.D. degree with the School of Engineering, Faculty of Science and Engineering, Manchester Metropolitan University, Manchester, U.K. He was a Lecturer with the Department of Electrical and Information Engineering, Covenant University. He was received the Best Graduating Student Award from the Department of Electronic and Electrical Engineering, Faculty of Engineering and Technology (FET) in conjunction with the Nigerian Society of Engineers (NSE). He has authored and coauthored more than 50 academic articles published in international peer-reviewed journals and conference proceedings. His research interests include wireless communications, machine learning, radio propagation modeling, the Internet of Things (IoT), cloud computing, and smart and connected cities. He is a member of the International Association of Engineers (IAENG). He is a Registered Engineer with the Council for the Regulation of Engineering in Nigeria (COREN).



**ABIGAIL JEFIA** graduated in information and communication engineering from the Department of Electrical and Information Engineering, Covenant University, Ota, Nigeria. In 2018, she was an Intern with TELNET Nigeria Limited as a Network Analyst/Engineer, where she honed her network management skills and gained deeper insights into the various advancements towards networking. In 2018, she received a Cisco Certified Network Associate Routing and Switching (CCNA Routing and Switching) Certificate from the experience garnered from her internships. In 2019, she gained an insight into machine learning and artificial intelligence based on her undergraduate thesis and applied techniques to develop a path loss model. She was also with the Omdena Community as a Data Wrangler to develop a model that would help cure Post Traumatic Stress Disorder (PTSD). She has authored and coauthored three international research articles. Her research interests include artificial intelligence, machine learning, data science, and the Internet of Things (IoT).



**ADEREMI A. ATAYERO** received the B.Sc. degree in radio engineering and the M.Sc. degree in satellite communication systems, in 1992 and 1994, respectively, and the Ph.D. degree from the Moscow State Technical University of Civil Aviation (MSTUCA), in 2000. He served as the pioneer Deputy Vice Chancellor (Academic), the Coordinator School of engineering, and twice as the Head of the Department of Electrical and Information Engineering. He is currently a Professor of communication engineering and the Vice Chancellor with Covenant University, Nigeria. He is also the Head of IoT-Enabled Smart and Connected Communities (SmartCU) research cluster. He has a number of scientific articles in International peer-reviewed journals and proceedings to his credit. His current research interests include communication engineering, including wireless sensor networks, wireless (mobile) communications, the Internet of Things (IoT), and smart cities. He is a member of other professional bodies and a COREN Registered Engineer. He was a recipient of various awards and scholarships including the 2009 Ford Foundation Teaching Innovation Award. He is on the Editorial Board of the Covenant *Journal of Science and Technology* and of several other International Journals.

**OGBEIDE KINGSLEY**, photograph and biography not available at the time of publication.



**NASIR FARUK** received the B.Sc. degree (Hons.) in physics from the Kano University of Science and Technology (KUST) Wudil, Nigeria, in 2007, the M.Sc. degree (Hons.) in mobile & high-speed telecommunication networks from Oxford Brookes University, Oxford, U.K., in 2010, and the Ph.D. degree in electrical and electronics engineering from the University of Ilorin, Nigeria, in 2015. In 2009, he joined the service of the University of Ilorin. From 2015 to 2016, he was a Postdoctoral Researcher with the Department of Communication and Networking, School of Electrical Engineering, Aalto University, Finland where he led the group that propose an energy efficient self-backhaul solution for future heterogeneous networks. He is currently a Senior Lecturer with the Department of Telecommunication Science and also the Deputy Director of the Joint Universities Preliminary Examinations Board, University of Ilorin, Nigeria. He has authored or coauthored more than 80 scientific publications. His current research interests include radio propagation, spectrum management, energy efficiency of access, and backhaul networks. He is a member of IET. He received numerous research grants and fellowships from the University of Ilorin, TETFUND, AFRINIC/FIRE, Dynamic Spectrum Alliance, Extensia Ltd., and IEEE. He has participated in the TPC of numerous international conferences.

**OLASUNKANMI F. OSENI**, photograph and biography not available at the time of publication.

**ROBERT O. ABOLADE**, photograph and biography not available at the time of publication.

...